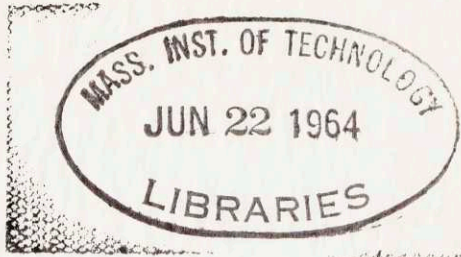


Thesis  
auth  
prof  
1964  
2.11



POSSIBLE METHOD FOR DETERMINING PARTICLE SIZE IN FOG FLOW

by

RICHARD LIBERACE  
B.S. Tufts University 1960

SUBMITTED IN PARTIAL FULFILLMENT OF THE REQUIREMENTS FOR THE DEGREE OF  
MASTER OF SCIENCE

at the

MASSACHUSETTS INSTITUTE OF TECHNOLOGY

May 21, 1964

**Signature redacted**

Signature of Author:..... Department of Nuclear Engineering

**Signature redacted**

Certified by:..... Thesis Supervisor

Accepted by:..... Chairman, Departmental Committee on Graduate Students

## POSSIBLE METHODS FOR DETERMINING PARTICLE SIZE IN FOG FLOW

38

by

RICHARD LIBERACE

Submitted to the Department of Nuclear Engineering of the Massachusetts  
Institute of Technology  
on May 21, 1964  
in partial fulfillment of the requirements for  
the degree of Master of Science

## ABSTRACT

The prospects of measuring particle size, velocity, and density distributions in fog flow was investigated. Experimental investigations concerning possible size distribution measurements were performed. No experimental determination of particle density or velocity measurements was attempted. These investigations considered two techniques utilizing fiber optics. One method measured the light attenuation due to a particle crossing a light beam, the other measured the quantity of light scattered by a water drop. Very simple systems such as colored water droplets produced from an atomizer spray and calibrated glass beads falling freely in air were examined. From measurements on these simple systems, it was concluded that the method measuring the quantity of directly scattered light from a water drop does not seem promising. The method of measuring the quantity of light attenuation shows some promise for measuring size distributions. Although only size distributions of glass beads ranging from 200 to 400 microns were measured successively, information gained in these tests show that future experiments employing better equipment might be able to measure size distribution between 30 to 70 microns. Since the experimental equipment was inadequate for measuring the size distributions in the colored water spray, it was concluded that judgement concerning the prospects of this method should be delayed.

Thesis Supervisor : Henri Fenech  
Title: Associate Professor of Nuclear Engineering

## ACKNOWLEDGEMENTS

The author is thankful to the Nuclear Engineering Department who made funds available for this work. Special thanks is due to Bill Hinkle, Dr. H. Fenech, Tom Green, and Dave Guinn.

## TABLE OF CONTENT

	page
ABSTRACT	ii
ACKNOWLEDGEMENTS	iii
TABLE OF CONTENT	iv
LIST OF FIGURES	v
LIST OF TABLES	vi
CHAPTER I Introduction	1
CHAPTER II The "Shadow" Method	4
a) Theory of Shadow Technique	4
b) Equipment	8
c) Experimental Procedure	22
d) Experimental Results	30
e) Discussion of Results	39
f) Conclusions	60
CHAPTER III The Light Scattering Method	
a) Theory	61
b) Apparatus	64
c) Experimental Procedure	70
d) Experimental Results	71
e) Conclusion	74
CHAPTER IV Suggestions For Future Work	
a ) Suggestions For An Improvement of "The Shadow Method"	75
b) Suggestion For An Improved Probe	76
REFERENCES	81

List of Figures

	page
Chapter 1	
1-1 Apparatus for Shadow Technique	2
1-2 Apparatus for Direct Light Scattering Technique	3
Chapter 11	
2-1 Shadow Technique	4
2-2 Light Intensity Variations as the Test Particle Passes the Light Field	5
2-3 Density Measurements	6
2-4 Arrangement of Equipment	9
2-5 Arrangement of Light Source	9
2-6 Probe Used to Measure Particle in the Range 200-400 $\mu$	12
2-7 Probe for Measuring Small Particles	14
2-8 Wiring of Photo-Tube	17
2-9 Block Diagram of Electronic Analysis Equipment	17
2-10 Signal Conditioner	20
2-11 Experimental Set-up Used to Test Linearity of Photo-Tube	23
2-12 Experimental Set-up Used to Determine Maximum Signal to Noise Ratio	23
2-13 Voltage at Which Photo-Tube Becomes Non-Linear vs. Applied Load Resistor = 2.2K	25
2-14 Maximum Signal to Noise Ratio Obtained vs. Applied Photo-Tube Voltage	25
2-15 Arrangement of Equipment Used to Measure Size Distribution of Glass Beads	27

	page
2-16 Set-up Used to Measure Water Spray Distribution	27
2-17 Size Distribution Measurements for Particle, C Type Glass Beads, Size Range 400-200 $\mu$	32
2-18 Size Distribution Measurements for Particle, H Type Glass Beads, Size Range 85-140 $\mu$	33
2-19 Size Distribution Measurements for Particle, R Type Glass Beads, Size Range 60 to 10 $\mu$	34
2-20 Size Distribution of Colored Water Spray	35
2-21 Normal Noise Spectra for Delay Time of 1000 and 500 sec D.C. Shift 1760 mv.	36
2-22 Photo of Pulses for Particle C Passing Through Probe # 1	37
2-23 Spray Experiment for Different Delay Times Based on 3469 Counts	38
2-24 Single Fiber Emitter Probe	39
2-25 Many Fiber Emitter Probe	40
2-26 Pulse Shape When a Particle Encounters a Broken Fiber	42
2-27 Details of End Surfaces of Light Pipes	44
2-28 Possible Particle Paths in Traversing the Light Pipe	45
2-29 Variations in Sensitivity of the Photo-Cathode Along Its Length	48
2-30 Variations in Sensitivity of the Photo-Cathode Across Its Projected Width in Plane of Grill	48
2-31 The Delay Time Effect	49
2-32 Examples of Edge Effects	54
Chapter 111	
3-1 Analyzing Device for the Direct Light Scattering Method	61
3-2 Expected Pulse from Photo-Tube	61
3-3 Experimental Set Up	68

	page
3-4 Black Box	68
3-5 Block Diagram of Electronic Equipment	69
3-6 Possible Receiver and Emitter Light Pipe Configurations	71
Chapter IV	
4-1 New Probe Design	76
4-2 Possible Paths a Falling Particle May Take	77
4-3 General Electronic Arrangement for New Probe	78

List of Tables

	page
2-1 Size of Glass Beads	21
2-2 Fraction of Particle Affected by Broken Fibers	43
2-3 Fractional Light Intensity Decrease	46
2-4 Fraction of Counts Missed Because of a Long Delay Time	50
2-5 Fraction of Counts Missed for Data Displayed in Fig. 2-25	51
2-6 Ratio of Expected Particles Pulse Height to D.C. Shift Pulse Height	52
2-7 Fraction of Particle Affected By Edge Effects	55
2-8 Major Non-Linear Factors	57
3-1 Table of Standard Equipment	65
3-2 Comparison of Light Sources	66



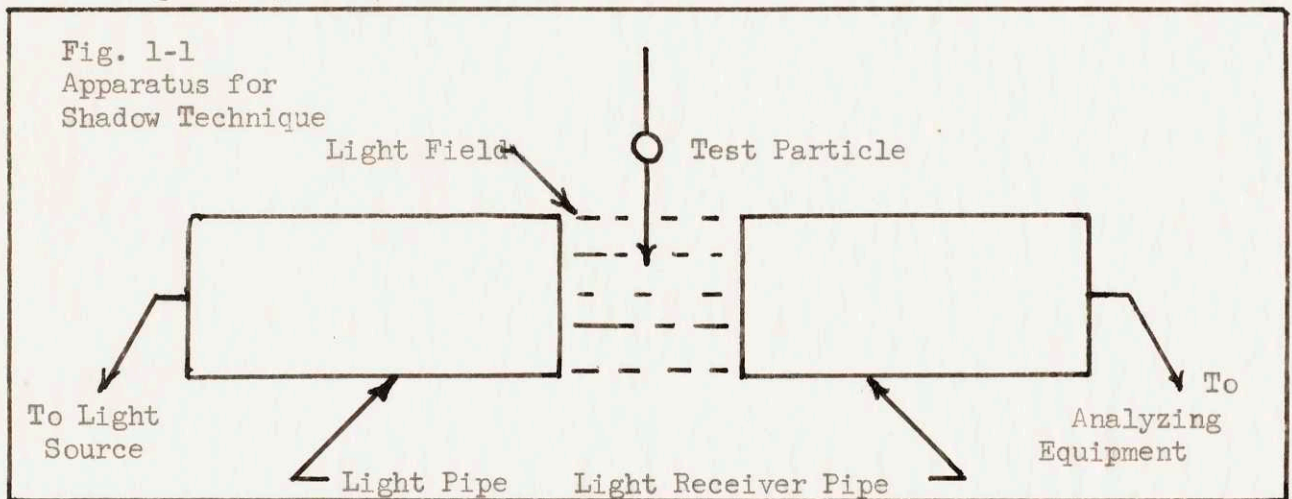
Chapter I  
Introduction

The purpose of this study is to investigate the use of two experimental methods for the determination of particle size, velocity, and density in fog flow. In such a flow the particle size can be of the order of 20-50 microns, the particle density can be of the order of  $10^8$  particles/ft<sup>3</sup>, and the particle velocity can be up to a few hundred feet per second. Information concerning the particle, size, velocity, and density can either prove or disprove current heat transfer theories and lead to better methods of predicting heat transfer in systems utilizing fog flow. Currently no one has been effectively able to measure all three parameters. Some experimenters have been able to measure the average particle size but not a particle distribution. The main difficulties originate with the flow perturbation produced by insertion of a probe inside the flow. As a result of this perturbation experimenters have tried to measure the fog parameter by using techniques whereby the experimental measuring apparatus has been located outside of the fog. Only limited success has been achieved.

The experiments described in this report utilized fiber optics in order to gather information so that a small probe which would not significantly effect a fog flow could be designed. The term fiber optics is used to denote a certain class of light transmitting fibers called light pipes. These flexible pipes contain bundles of single

fibers whose diameter may be as small as  $0.3\mu$ . These pipes can be arranged in a suitable apparatus to measure the light attenuation of a particle as it crosses a light beam or the amount of light scattered by a test particle.

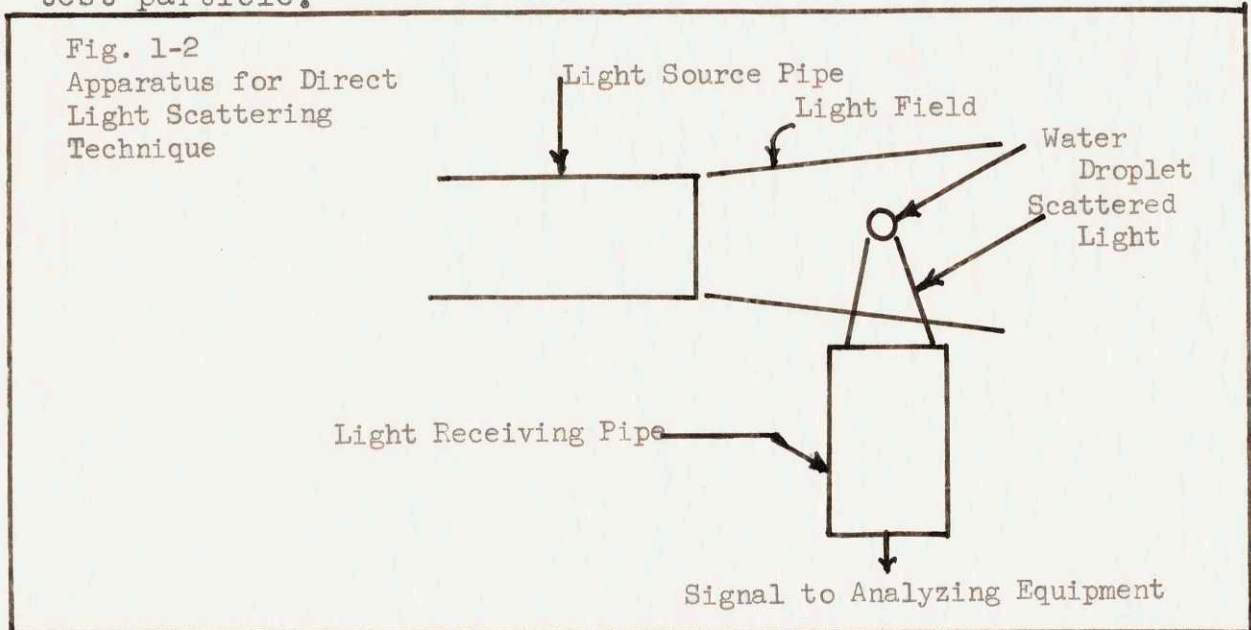
The method described in Chapter 2, called the shadow technique, consists of measuring the decrease in light intensity as a colored water drop or glass bead passes through a light beam. Figure 1-1 shows the arrangement of the light pipes in this instance .



This figure shows two light pipes arranged so that the light beam from one flows into the other. Auxiliary equipment not shown consists of equipment capable of producing a light beam and capable of analyzing any light collected. As the opaque test particle traverses the light field, a shadow is produced on the receiver system. From a measurement of the light intensity decrease the size of the particle may be determined.

The method found in Chapter 3 measures the amount of

light scattered by a small water droplet. An arrangement for this method is shown in Figure 1-2. Light from the source striking the particle as it enters the light field is partially scattered. The amount of scattered light collected by the receiving system can be related to the size of the test particle.



For years similar methods for particle size determination have been used by meteorologists, chemists, astronomers, and workers in other fields of science. The shadow technique has been used by meteorologists in the determination of rain drop sizes. Methods for the measurements of the direct light scattering have been employed by researchers ( Ref. 1,2,3 ) who measured particle density and size distribution for very low density fog.

Neither method has been used to measure the fog parameters under the above listed fog flow conditions.

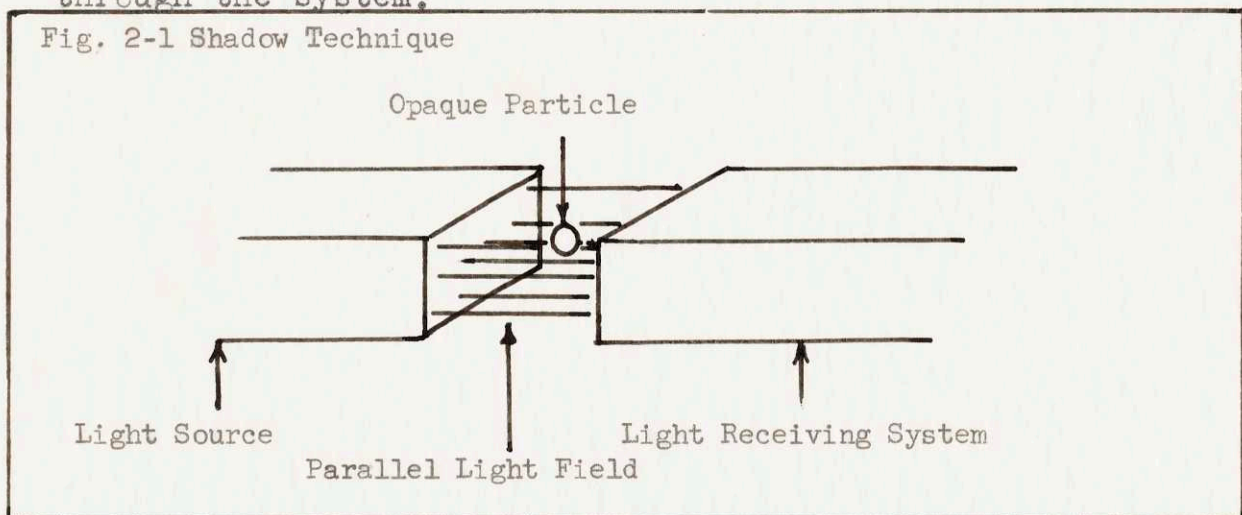
Chapter 11

The "Shadow" Method

### Theory of the Shadow Technique

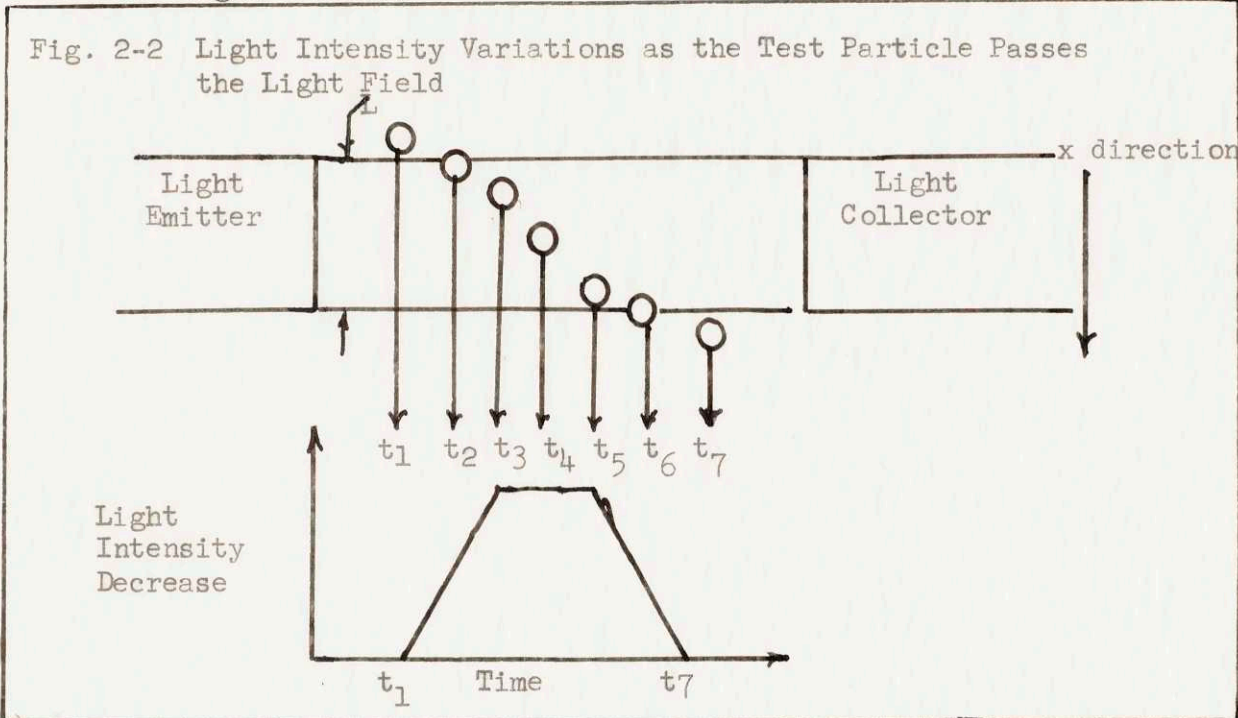
The theory concerning the "shadow technique" can be illustrated with the aid of Fig. (2-1) which shows a light source emitting a uniform parallel beam of light collected by a receiving system. When a partially opaque particle travels through the light field, the light intensity reaching the receiver system is diminished.

This light intensity decrease is proportional to the cross sectional area of the shadow cast by the particle. Since any orthographic projection of a sphere is a great circle, the area of its' shadow is directly related to its' size if diffraction and edge phenomena are neglected. Therefore, measurement of the light intensity decrease will yield information on the size of a spherical particle passing through the system.



The velocity of the particles in a specific direction may be determined by measuring the total time the light intensity has been diminished and the width of the light

beam in that particular direction. Fig. 2-2 shows the variation of light intensity as a function of time as a particle traverses the light field. Distance  $L$  is the thickness of the light field.

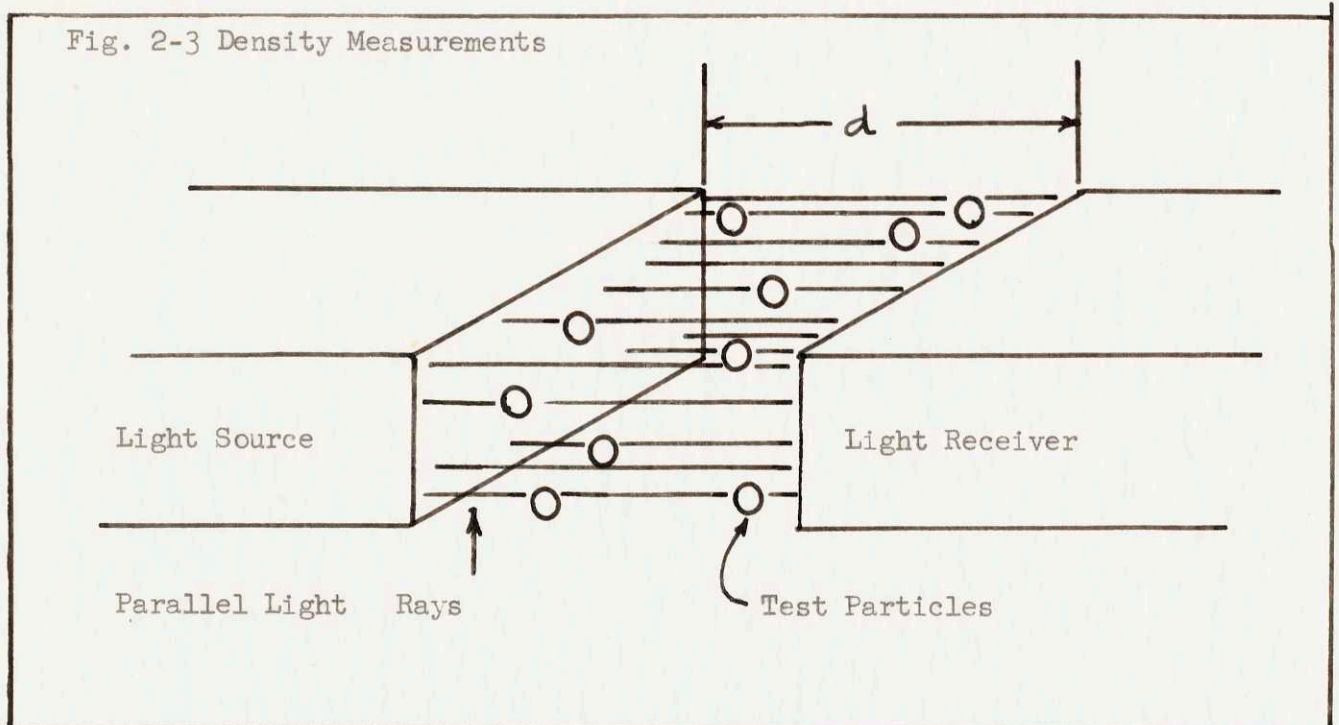


When the particle is at position  $t_1$  it has not yet entered the light field and the light intensity has not decreased. Position  $t_2$  shows a particle entering the light field. The intensity is gradually decreasing until the particle fully enters the light field at which time ( $t_3$ ) the light intensity change remains constant. The light intensity change remains constant ( points  $t_4$  ,  $t_5$  ) until the particle emerges from the light field at time  $t_6$ . At this time the light intensity starts to increase to its initial value at time  $t_8$  when the particle is completely out of the light beam. Once  $t_1$  and  $t_7$  have been measured the  $x$

direction velocity is given by eq. (1)

$$V_x = \frac{L}{t_7 - t_1} \quad (1)$$

Density measurements are possible for both opaque or partially opaque objects. In the case of opaque objects in a high density flow true density measurements are difficult, since particle overlap becomes a serious problem. For partially opaque objects good density measurements can be made provided enough samples are taken for a valid statistic representation. The physical size of the light probe should be small enough so that the flow characteristic under study will not be perturbed.





The determination of the particle density requires knowledge of the size distribution, since the light absorption coefficient as a function of particle size must be known. Values for this coefficient for water drops are listed in (Ref 1). Once this absorption coefficient is known and the spatial distribution of particles is assumed to be random within the light field, the light intensity reaching the receiver system can be represented by eq (2)

$$I = I_0 e^{-knd} \quad (2)$$

where  $I$  = the light intensity reaching the receiver system (ergs / cm<sup>2</sup> sec)

$I_0$  = the initial light intensity from the light source (ergs / cm<sup>2</sup> sec)

$k$  = the total absorption coefficient (cm<sup>-1</sup>)

$n$  = the density of particles in the light beam  
(  $\frac{\text{particles}}{\text{cm}^3}$  )

$d$  = the distance between the light source and light receiver (cm)

The value of  $k$  is given by

$$k = \sum_i \frac{n_i}{n} \lambda_i \quad (3)$$

where  $\frac{n_i}{n}$  = the fraction of particles measured in the  $i'$  th groups

$\lambda_i$  = the absorption coefficient for particles in the  $i'$ th groups.

After measuring the values of  $I, I_0, d$ , and the size distribution,  $k$  may be computed and the value of  $n$  determined from eq (2).

## Equipment

The equipment can arbitrarily be classified into three groups, 1) optical measuring equipment, 2) the electronic analysis equipment, and 3) miscellaneous materials. The measuring equipments contain the necessary apparatus for detecting the test particle. The analysis equipment is used to analyze the optical signals produced. The third group consists of the glass beads that were analyzed and the atomizer used to produce the water spray. Following is description of the three groups.

### 1) Optical Measuring Equipment

The arrangement of this equipment is shown in Fig. 2-4. Light from a lamp is condensed and transmitted through a light pipe. The emergent light beam is collected by a receiver light pipe which transmits this light signal to a photomultiplier tube.

A probe was constructed to hold the light pipes in the correct position and to provide a covering with a slit opening, receiver pipes. A narrow opening at the top of the probe allows test particles to be introduced into the light beam.

### Light Source

The light source used was a 21C.P. tungsten filament autohead lamp powered by 6 volts D.C. source. A filament lamp was used since other types of light sources such as

Fig 2-4  
Arrangement of  
Equipment

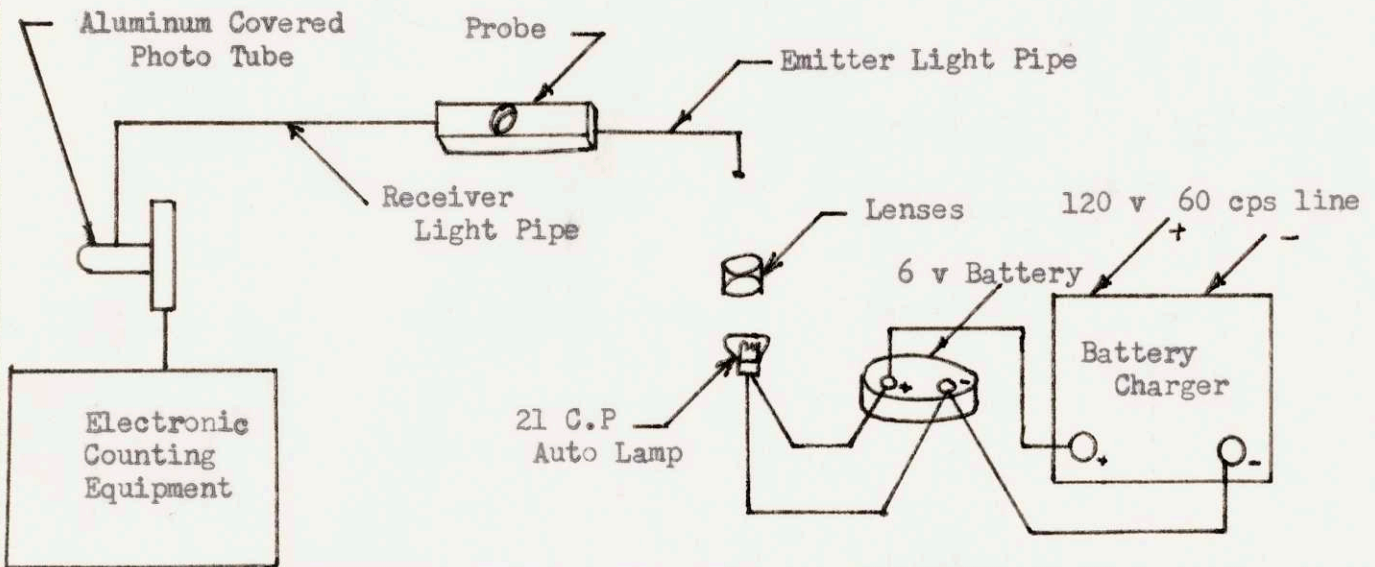
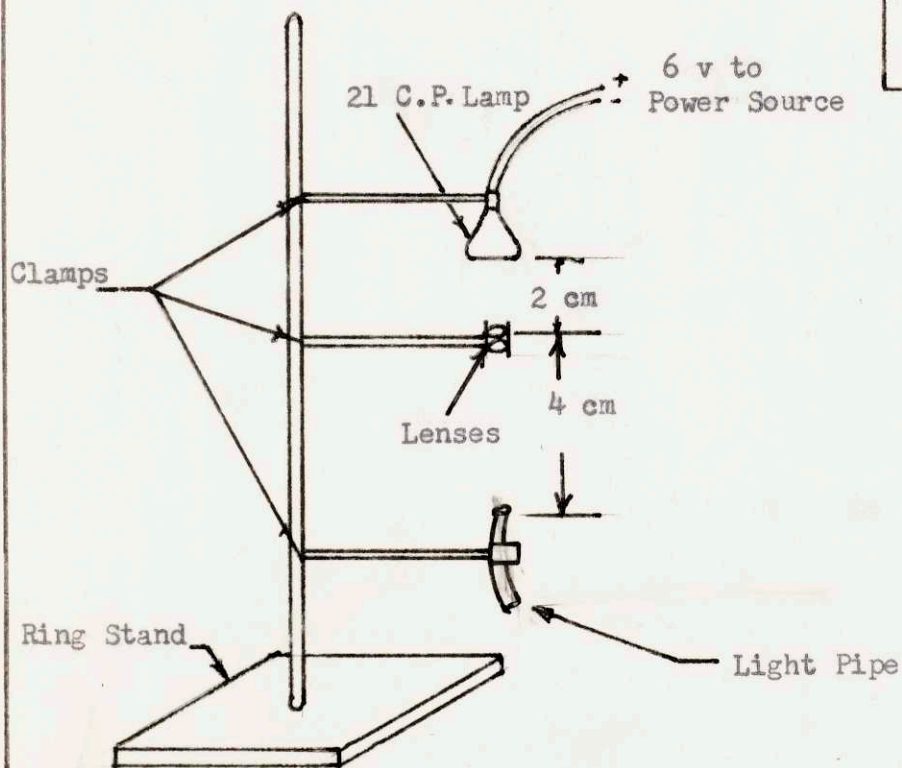


Fig 2-5  
Arrangement of  
Light Source



Note:  
Drawn not to scale  
or in proper  
proportions

xenon lamps and arc lamps which are more intense and easily focused were not available.

In operating the light source care had to be taken to insure that the applied voltage remained constant for consistency in the experiments. This is because different applied voltages produce different light spectra from a tungsten filament, and the sensitivity of a photomultiplier tube varies with wave length. Also, variations in the applied voltages produce undesirable variations in light intensity. A D.C. supply was used rather than an A.C. supply in order to eliminate a source of power frequency noise.

The D.C. current was supplied by a battery charger connected in parallel with a storage battery. This arrangement yielded a voltage ripple of less than 1%.

#### Light Collecting System

The purpose of this system is to collect and focus the light from the tungsten lamp. This is accomplished by the use of two identical double convex lenses. Each is 24 mm in diameter with a 22.1 mm focal length. The set-up is shown in Fig. 2-5. The image was not sharply focused on the end of the light pipe since a sharply focused plane in space would provide regions of varying light intensities, the result of the spiral shape of the thin tungsten filament. A sharply focused image of the filament wire would be very intense while points just off the image would have lesser

intensity. A diffusely focused image will provide a space region of almost uniform intensity.

### Light Pipes

The purpose of the light pipes is to transmit light. As depicted in Fig 2-4, light from the source is transmitted through one pipe and collected by the other pipe. The pipes consist of fifty to sixty fibers, each  $75\mu$  in diameter and 38" in length. The cross section of each pipe is circular with a diameter of 1 mm and an effective area of  $2.6 \times 10^{-3} \text{ cm}^2$ . Approximately 50% of the incident light is absorbed in each 5 foot length of pipe. Also, since 10 to 20 per cent of the fibers used were broken, the frontal area, and therefore the amount of light transmitted, was reduced by that amount.

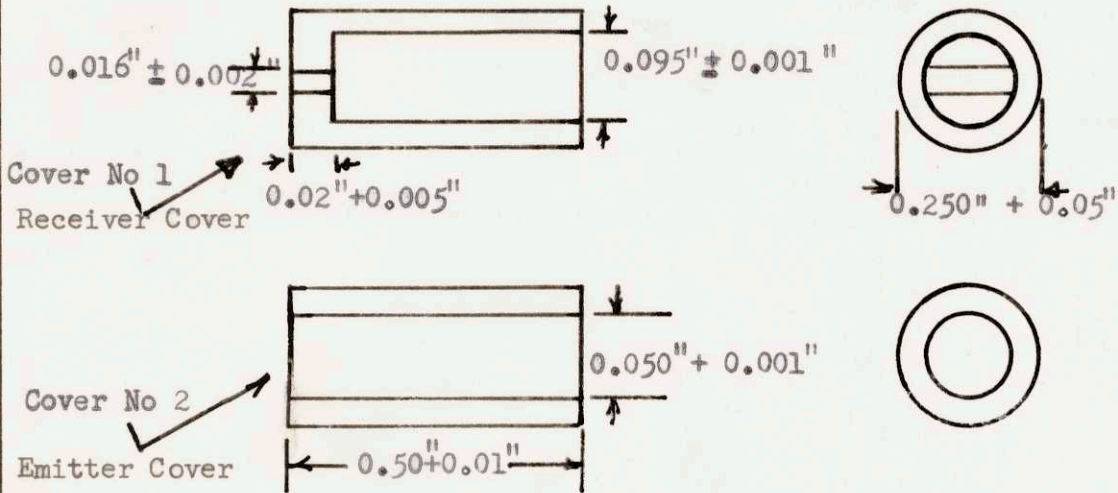
### Probe

The probe is a metallic object which holds the emitter and receiver light pipes in a rigid position. It provides an opening for particles to pass through the light field and includes a narrow slit opening for the receiver light pipe.

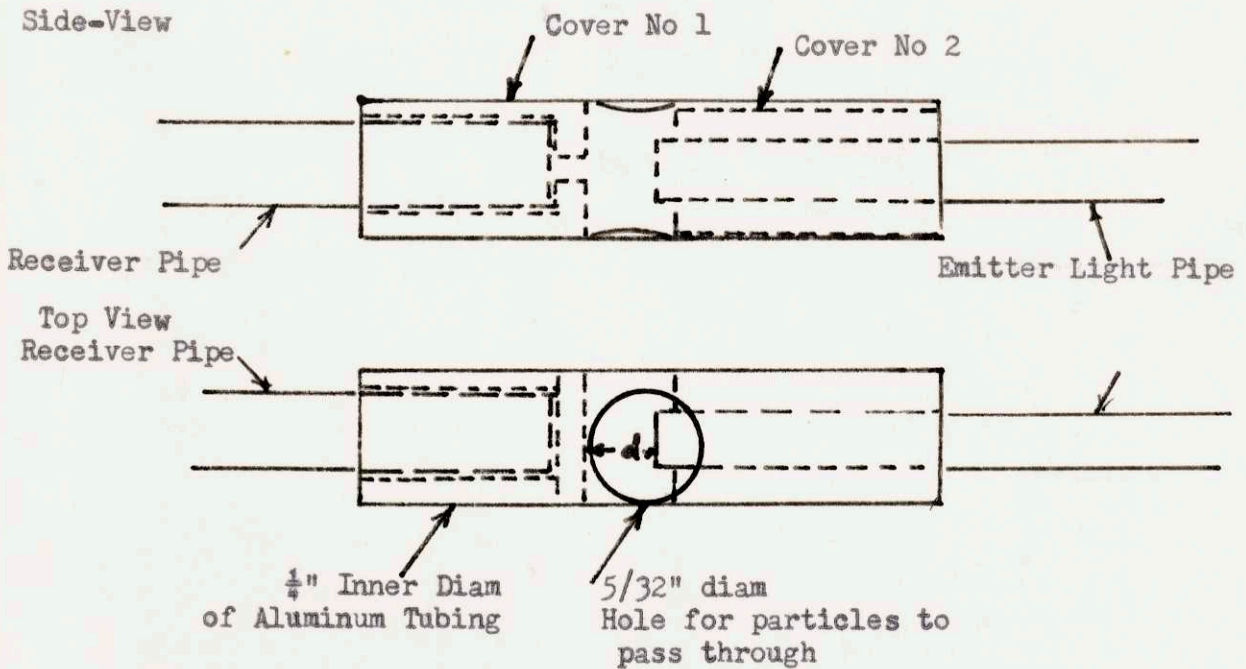
Two different probes were used. The initial probe, shown in Fig 2-6 consists of a section of  $\frac{1}{4}$ " inside diameter aluminum tubing and two cylindrical light pipe holders. Enough clearance was provided between the holder and pipe so that the pipe could be easily moved in and out of the holder. The clearance between the two holders and the outer aluminum tube is small enough so that very slight pressure applied on the outer tube will fasten the two holders in a rigid position which will remain fixed throughout the course of experiments.

Fig 2-6  
 Probe #1 Used to Measure  
 Particles in the Range  
 200 - 400  $\mu$

LIGHT PIPE COVERS



PROBE ASSEMBLY

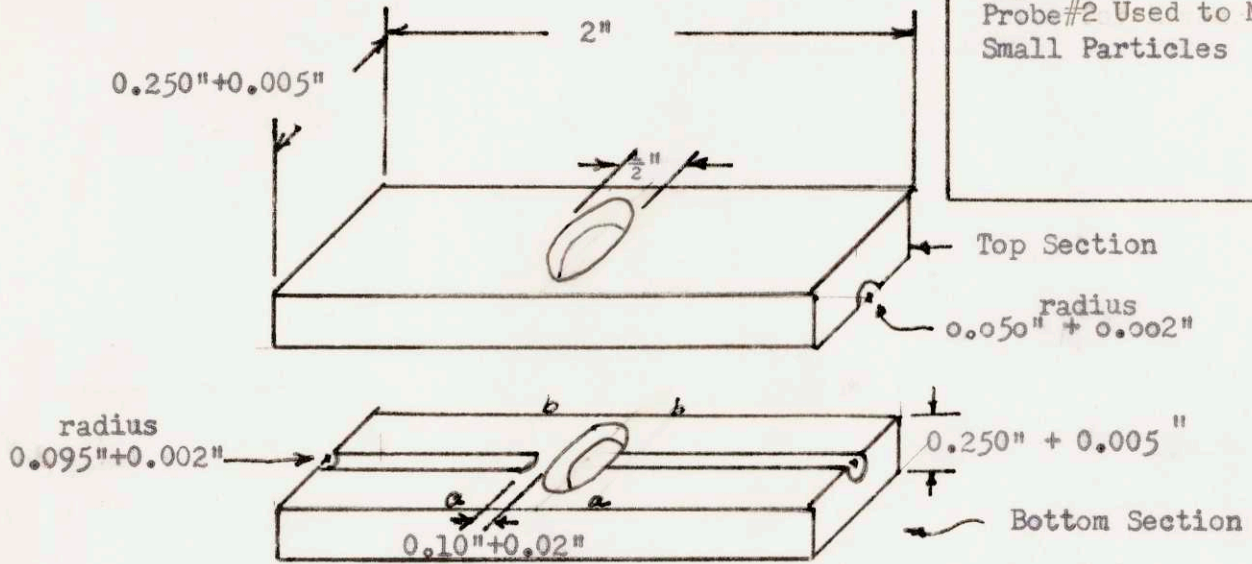


The construction of this probe is as follows:

- 1) The inside of the aluminum tubing is machined to  $0.250 \pm 0.005$ ,"
- 2) The pipe holders are made from  $\frac{1}{4}$ " aluminum rod which are machined to  $0.245 \pm 0.004$ ,"
- 3) A hole of  $0.050 \pm 0.001$ " diameter is drilled through the emitter holder.
- 4) A 0.016" diameter cutting saw is used to cut a narrow slit of 0.03" deep through the center line of the receiver holder.
- 5) A hole of  $0.095 \pm 0.002$ " diameter is drilled through the receiver holder down to the slit opening.
- 6) The holders are sanded with emery cloth and fitted into the tube where they are permanently made fast by pinching the outside of the tube.
- 7) The light pipes are inserted into the holders until they are the desired distance apart.
- 8) Small washers of black electrical tape are made with an inner diameter equal to the diameter of the light pipe and an outer diameter equal to 0.25". These fit snugly into the aluminum tubing and prevent the pipes from moving.
- 9) To make sure the assembly remains rigid, the end of each pipe is taped to the aluminum tubing.

The second probe is shown in Fig 2-7. It was designed to measure smaller particles than the previous one and to provide

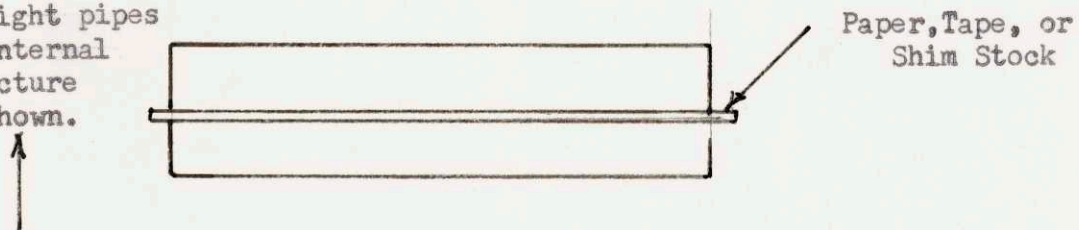
Fig 2-7  
Probe #2 Used to Measure  
Small Particles



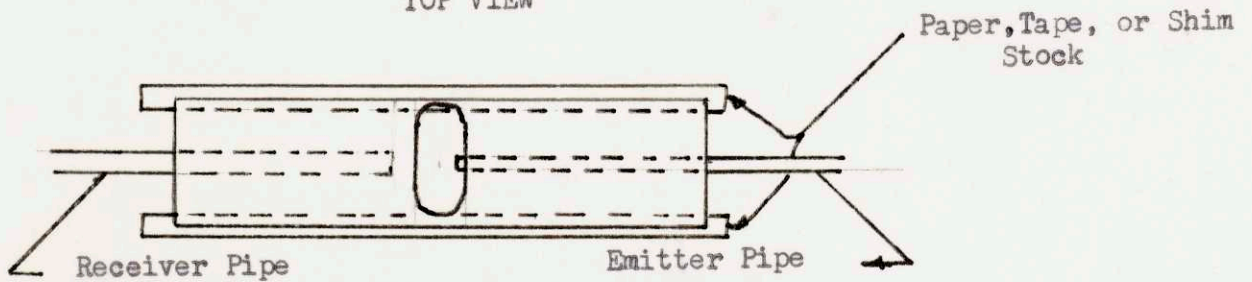
Probe with paper or shim stock or tape inserted to make the slit opening.

SIDE VIEW

No light pipes  
or internal  
structure  
is shown.



TOP VIEW





a means of varying the slit opening of the receiver pipe.

This probe consists of two pieces of machined No. 1100 aluminum, placed together. Openings for both the receiver and emitter pipes are provided as well as a narrow opening through which test particles may fall. The slit is made by placing two strips of thin material between the aluminum pieces. These strips should be placed along the full length of the probe so that neither light pipe is blocked by the strips and so that the particle flow is not interrupted. The slit has width approximately equal to the diameter of the light pipe and a height equal to the strip thickness.

Shim stock can be used for the strips, since its thickness is uniform and can be as small as 0.001". However the problem of removing cutting burrs makes this stock somewhat undesirable.

Paper can also be used as strips since its thickness is uniform. Paper has the undesirable property of absorbing water which causes its thickness and width to vary. Scotch tape, which has a uniform thickness of 0.0018" (45.6 $\mu$ ), was chosen as the strip material for the probe which was built. This material is easy to handle and does not lose its shape when in contact with water. Different slit thicknesses are obtained by using a number of layers of tape.

The most accurate method of varying the slit opening is by electro-plating. After covering the central region of the probe from point a to point b with black electrical tape, each probe section is emersed in an electroplating solution and a

metallic thickness whose variation may be controlled within 50 millionths of an inch is deposited on the exposed metallic surfaces. A slit of thickness equal to the thickness of deposited metal will result when the probe is reassembled.

In the original design, the emitter and receiver light pipe terminate 0.03 inches from the slot opening where the test particles flowed. The beam from the emitter pipe passes through an opening with dimensions similar to those of the opening of the receiver pipe. Since the distance between the two pipes is 20 times greater than the height of the slit, the light beam entering the emitter pipe is almost parallel in the vertical direction. Unfortunately an error in manufacture prevented testing this design.

## 2) Electronic Analysis Equipment

The purpose of the electronic analysis equipment is to measure and record the magnitude of the observed pulses. Fig. 2-9 is a block diagram of this equipment. The output signal from the photo tube is fed into an oscilloscope, then through a signal conditioner and finally into a pulse height analyzer.

### Photo-Multiplier

The purpose of the photo-multiplier tube is to receive the light from the light pipes and convert it into an electrical signal. An RCA 931A photo-tube whose characteristics are listed in Ref. 5 was used.

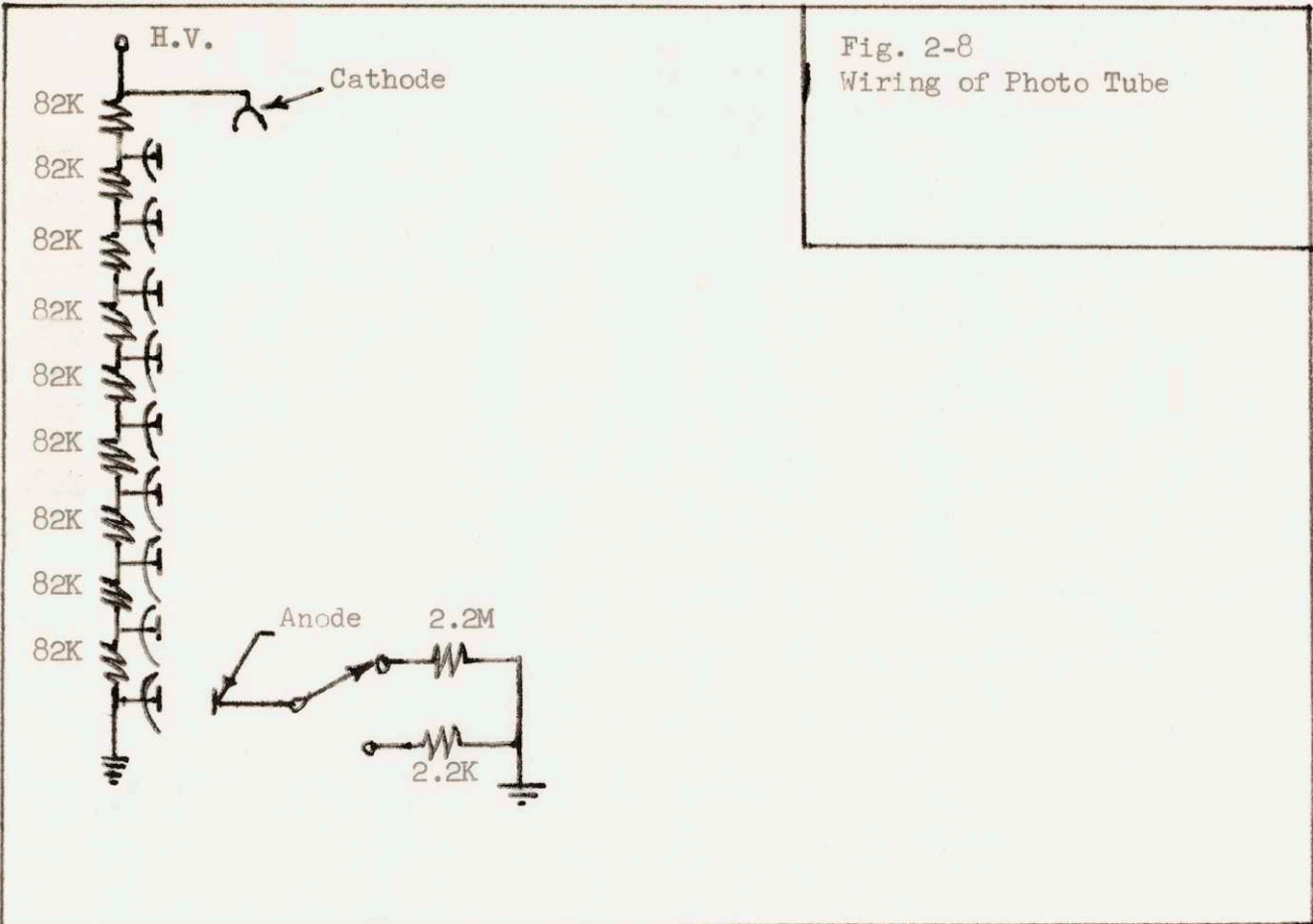


Fig. 2-8  
Wiring of Photo Tube

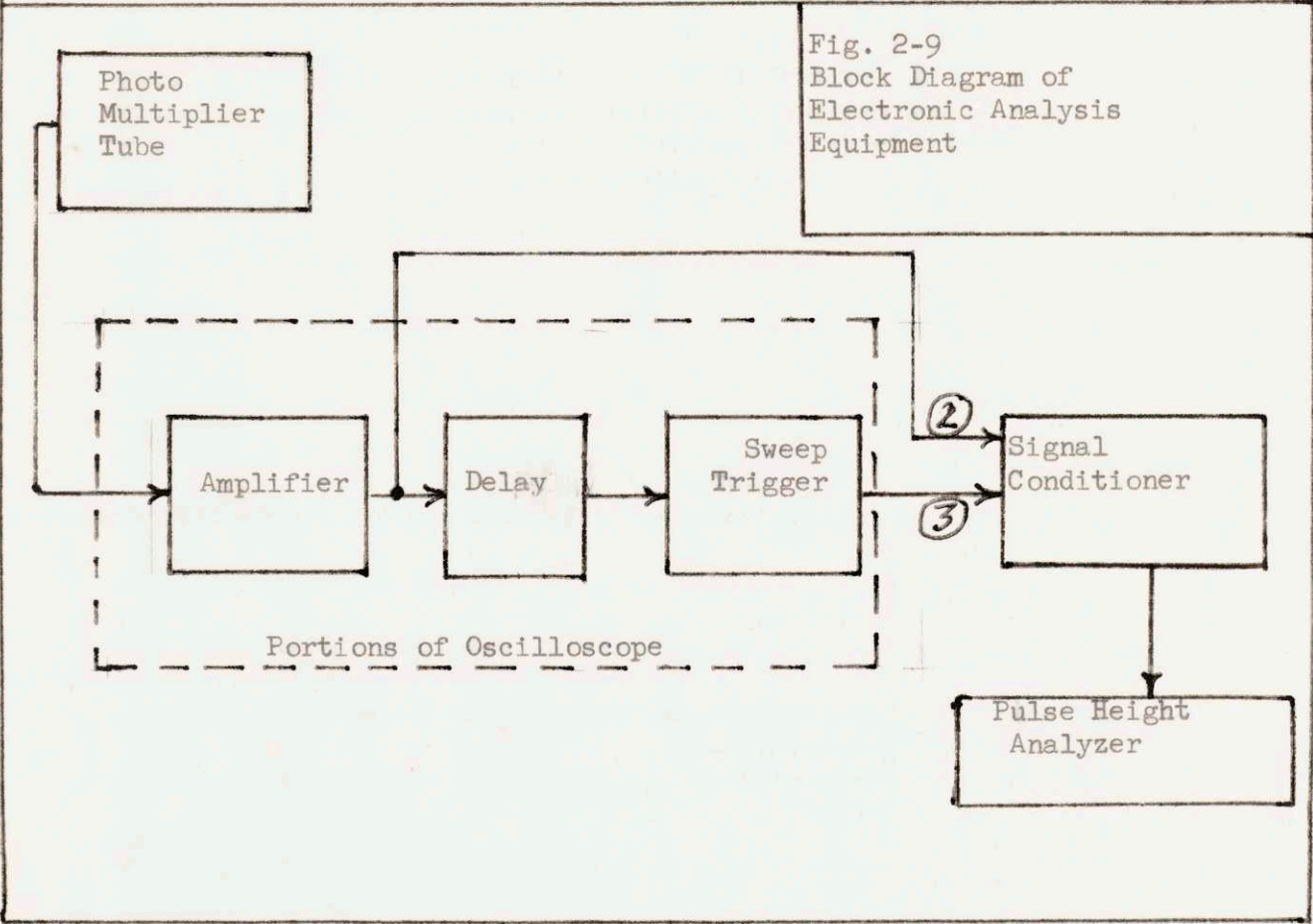


Fig. 2-9  
Block Diagram of  
Electronic Analysis  
Equipment

The tube wiring, shown in Fig.2-8, is of such a nature that the response remains linear for the largest quantity of light, incurred in an experiment, that strikes the photo cathode. Usually, 500 K resistors are connected between dynodes of a photo tube. In this set up, 82 K values are used to cause a larger current to flow through the resistors. The result of a large current flow between dynodes is that changes in current due to light intensity changes will cause less percentage variation in dynode current and hence dynode voltage. Therefore the overall tube gain which depends upon the individual dynode voltages will vary less.

Experiments performed at an overall tube voltage of 830 v. showed that the photo-tube maximum output signal voltage for linear operation increased from 1500 mv to 2700 mv when the smaller resistors were employed.

Two load resistors, one 2.2 K and the other 2.2 M are connected to a switch so that either can be used. The 2.2 M resistor should be used for weak pulses whose period is greater than  $10\mu$ . The 2.2 K resistor can be used for pulses as short as  $10\mu$  sec. but requires a stronger signal than that for the 2.2 M resistor. An aluminum shield covers the photo tube except for a small opening through which the emitter light pipe is placed. This shield prevents external electric fields from interfering with the operation of the photo-multiplier tube. These external fields are mostly radio waves and 60 cycle waves.

## Oscilloscope

The oscilloscope is a model 545 with a type L plug in unit manufactured by Textronic Inc. of Portland Oregon.

The oscilloscope provides an amplifier for the phototube output pulse and a delayed trigger for the signal conditioner. The cathode ray tube display portion of the scope is not used as part of the analysis equipment.

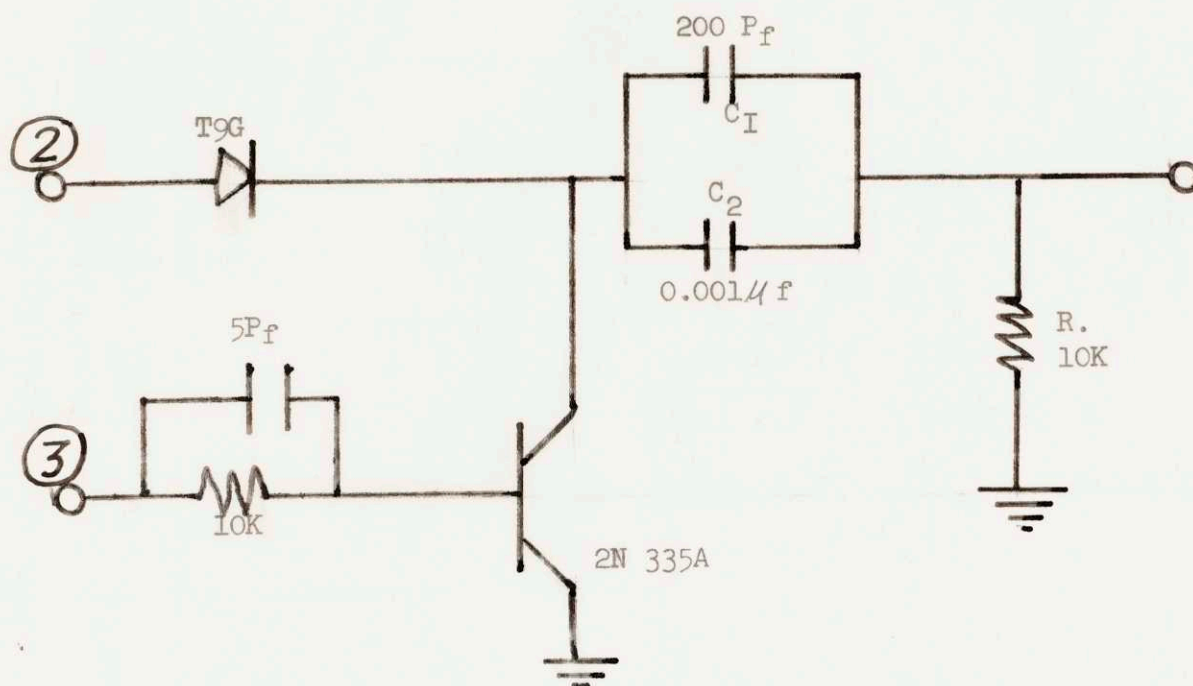
## Signal Conditioner \*

The purpose of the signal conditioner is to convert the slow positive signal pulses to pulses with fast (negative) rise time with the same amplitude as the signal pulses. This fast rise time is needed for the operation of the pulse height analyzer. The schematic of this conditioner is shown in Fig. 2-10.

Its operation is as follows: The transistor is normally not conducting, so that when a signal arrives from the oscilloscope amplifier it charges capacitors  $C_1$  and  $C_2$  through the diode and resistor  $R_1$ . The capacitors charge to the maximum amplitude of the signal then are held there due to the high back resistance of the diode. At the appropriate time, a positive trigger pulse is received from the oscilloscope which turns on the transistor, quickly discharging  $C_1$  and  $C_2$ . At the output appears a negative going pulse of fast rise time with amplitude equal to that of the signal.

\* Developed by Mr. D. Gwinn of the M.I. T. Nuclear Reactor  
Electronic Shop

Fig. 2-10  
Signal Conditioner



Note : Points ② and ③ connect with points ② and ③ in Fig. 2-9

### Pulse Height Analyzer

This analyzer is a 256 channel device manufactured by Technical Measurements Corp. of New Haven, Conn. It is ordinarily used to analyze fast nuclear pulses.

### 3) Experimental Sample Materials

Two types of particles were used to test the equipment; glass beads and water droplets.

The glass beads are small glass spheres whose diameter ranges from 10 to 400  $\mu$ . These are manufactured by Prismo Safety Corp. in Harrington, Pa. Three size ranges of particles were obtained. These size groups are called C, H, and R. Table 2-1 lists the size range of each group.

The water droplets were produced by an atomizer manufactured by De Vebbis of Somerset, Pa. Life perserver dye was added to the water used in this atomizer in order to produce a colored spray.

Table 2-1 Size of Glass Beads

Particle Group	Size Range
C	420-200 $\mu$
H	149-105 $\mu$
R	44-10 $\mu$

### Experimental Procedure

The experimental procedure can be divided into two parts:

- 1) an initial inspection of the electronic and subordinate equipment, and
- 2) size distribution measurements of both glass beads and water spray.

#### 1) Check of Electronic Equipment

Each individual piece of electronic equipment was routinely checked before assembling the equipment. This check was accomplished by connecting a calibrated signal to the input of each component and noticing the form of the output signal. The equipment was then assembled as shown in Fig 2-9 and Fig 2-4, and all connections checked for shorts or open circuits. As a further check on the system, a light signal was applied to the input and the output pulse forms were observed on an oscilloscope. Both the light beam from the stroboscope and the D. C. signal from the auto-head lamp were used.

The photo-tube cover was checked for light tightness by covering the exposed end of the receiver pipe and flashing a light beam from a stroboscope on the photo-tube cover. Any leaks would have allowed this intense ( one million candle power ) beam to produce pulses which would have been detected by the pulse height analyzer. The strobe was not put near the photo-tube since the magnetic field produced by the strobe flash would affect the response of the photo-tube.



Fig 2-11  
 Experimental Set - Up  
 Used to Test Linearity  
 of Photo Tube

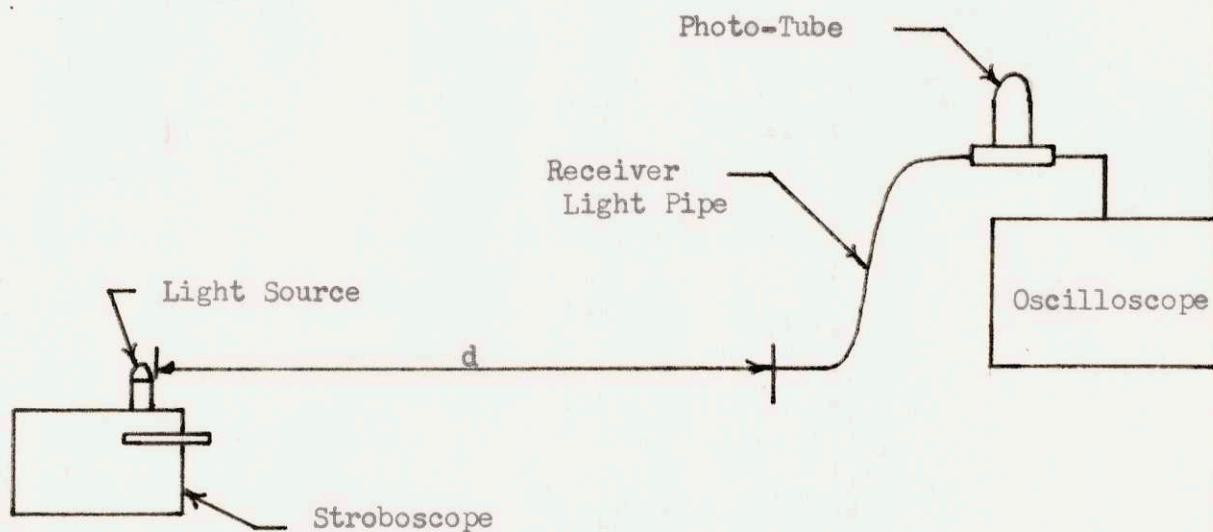
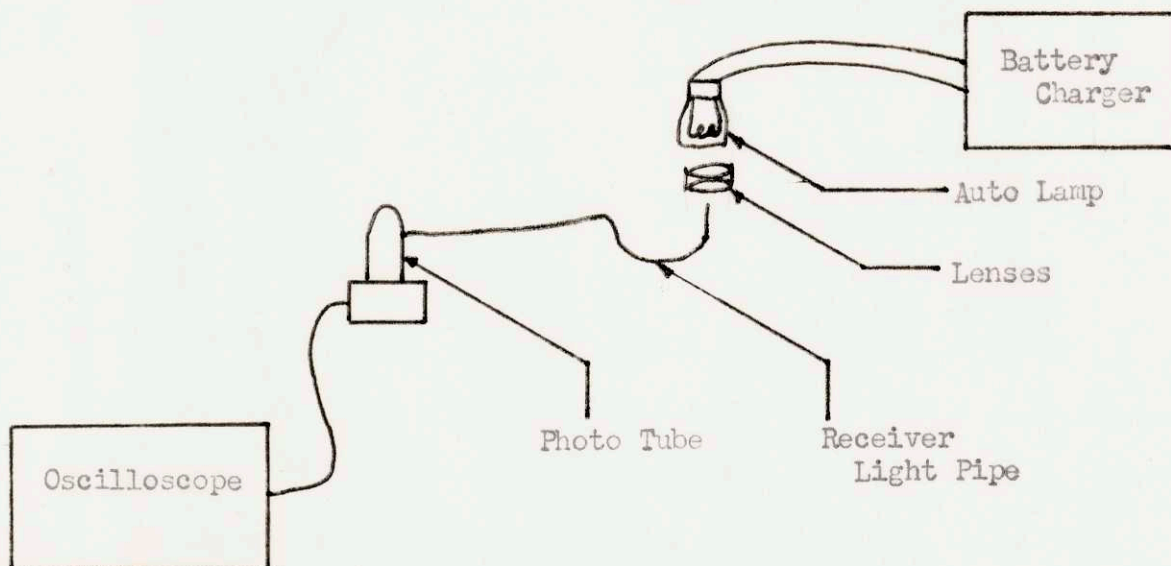


Fig 2-12  
 Experimental Set - Up  
 Used to Determine  
 Maximum Signal to  
 Noise Ratio

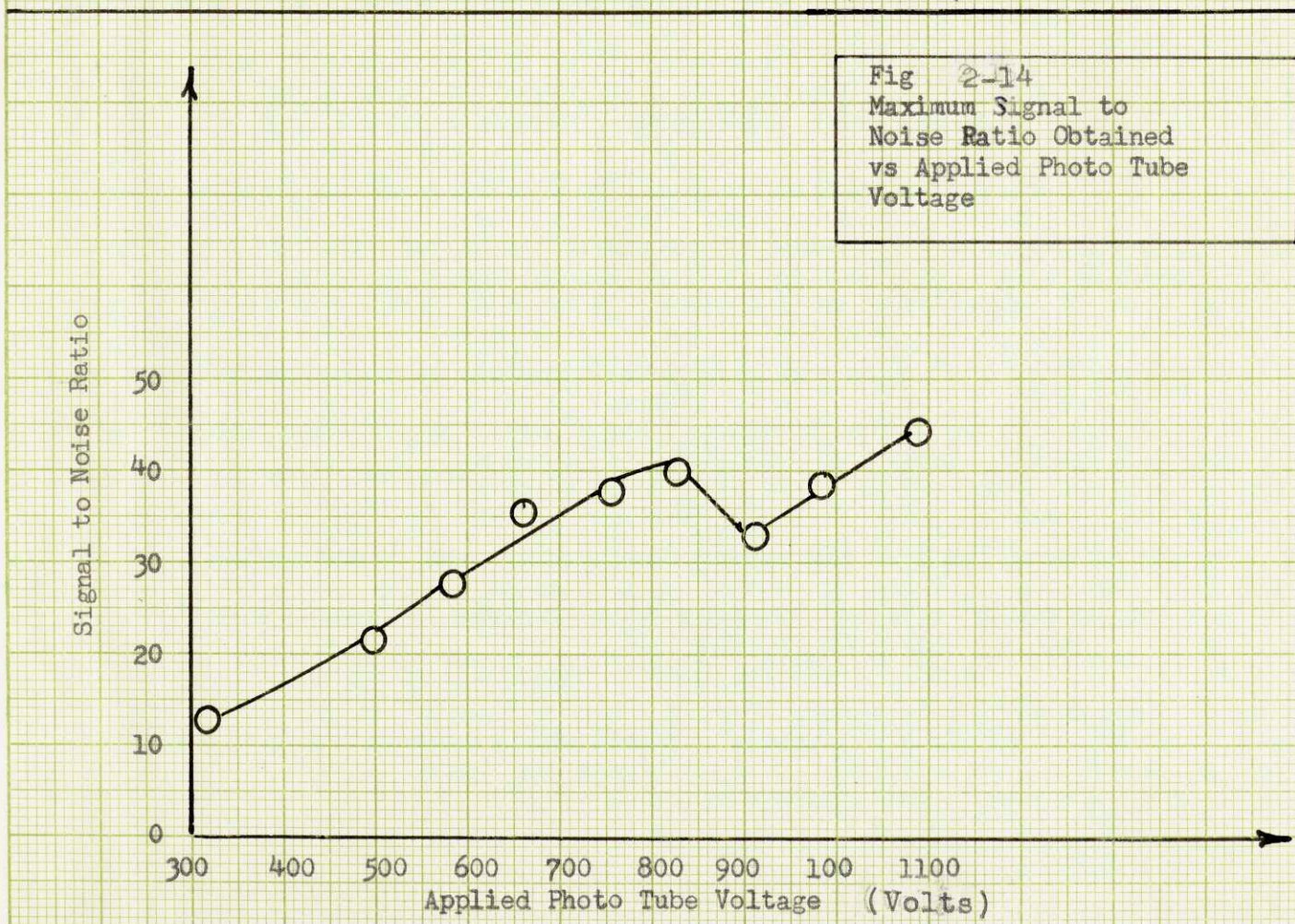
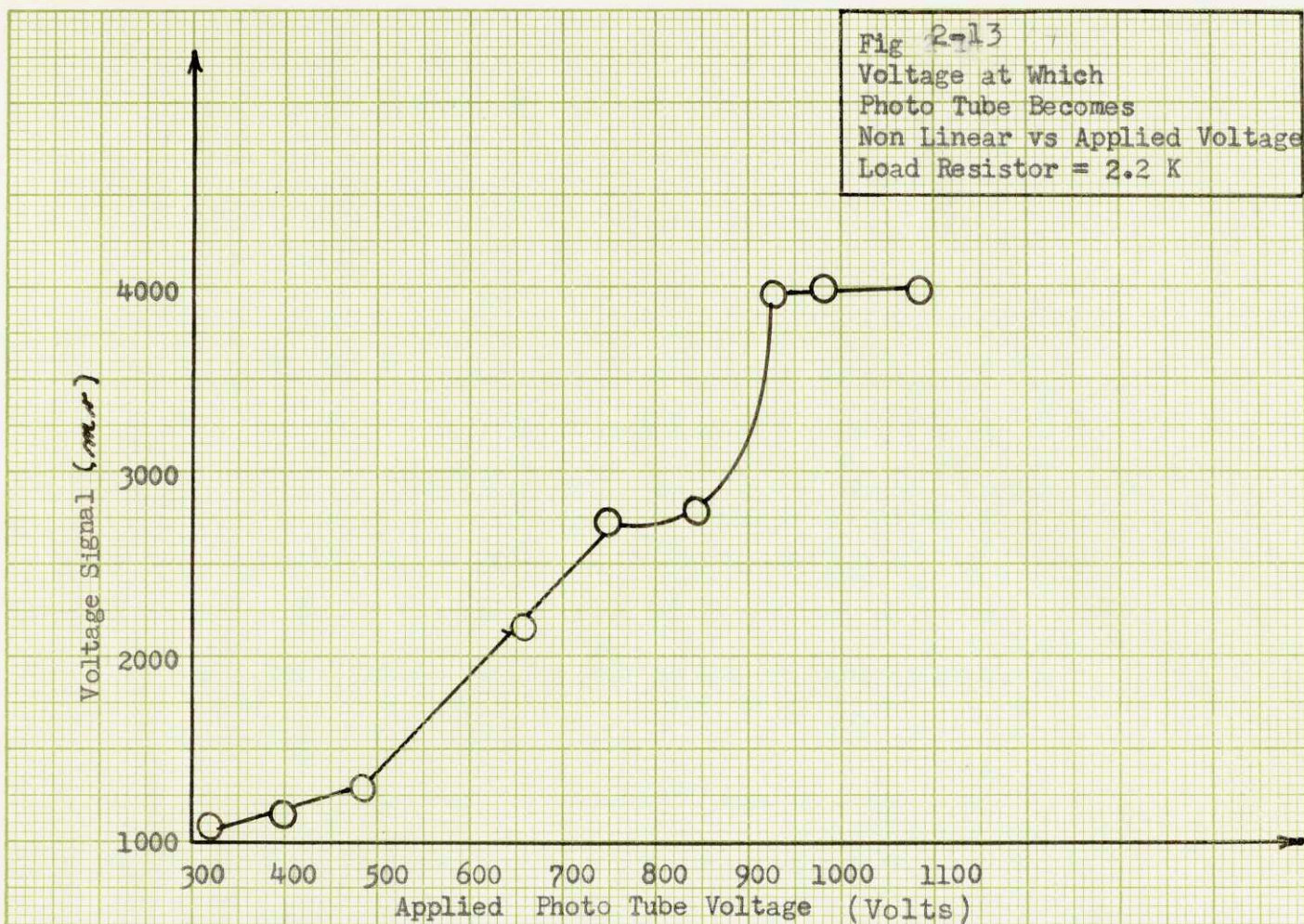


After the equipment was properly checked, the maximum quantity of light reaching the cathode which caused the photo tube to operate in a non-linear manner was determined. The photo tube operates in a non-linear manner when the magnitude of the light intensity is not directly proportional to the output voltage of the photo tube. To find this value of light intensity, use was made of the fact that the light intensity from a point source varies inversely as the square of the distance from the source. The equipment set-up for this measurement is shown in fig 2-11. The light flash from the stroboscope is about 1 cm in width and 0.2 cm in height and can be considered a point source at distances greater than one meter.

The distance from the light flash to the receiver light pipe was varied and the output voltage of the photo-tube was measured by means of an oscilloscope. At distances greater than 10 meters the response of the photo-tube showed a  $1/r^2$ . Fig 2-13 shows the maximum signal output voltages (for a given D. C. supply voltage) at which the tube behaves in a linear manner.

The rest of the electronic apparatus was checked to make sure it was linear for the signal levels at which the photo-tube was linear.

After the limits of linearity were observed the maximum signal to noise ratio was determined. The dominant noise in this case was due to current variations between the dynodes rather than to dark current. Noise measurements were made with the apparatus arranged as shown in Fig. 2-12. The results obtained are shown



in Fig. 2-14.

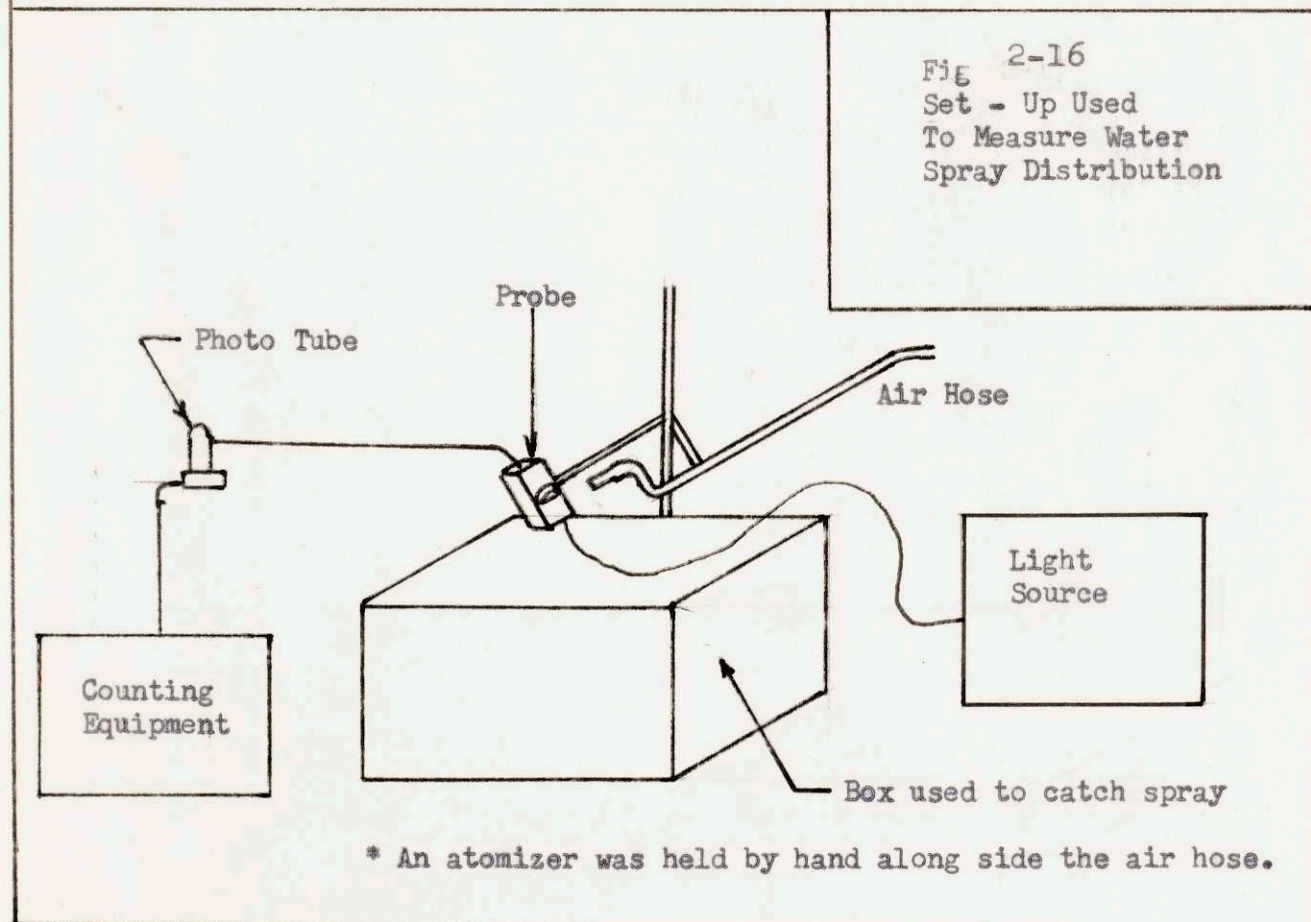
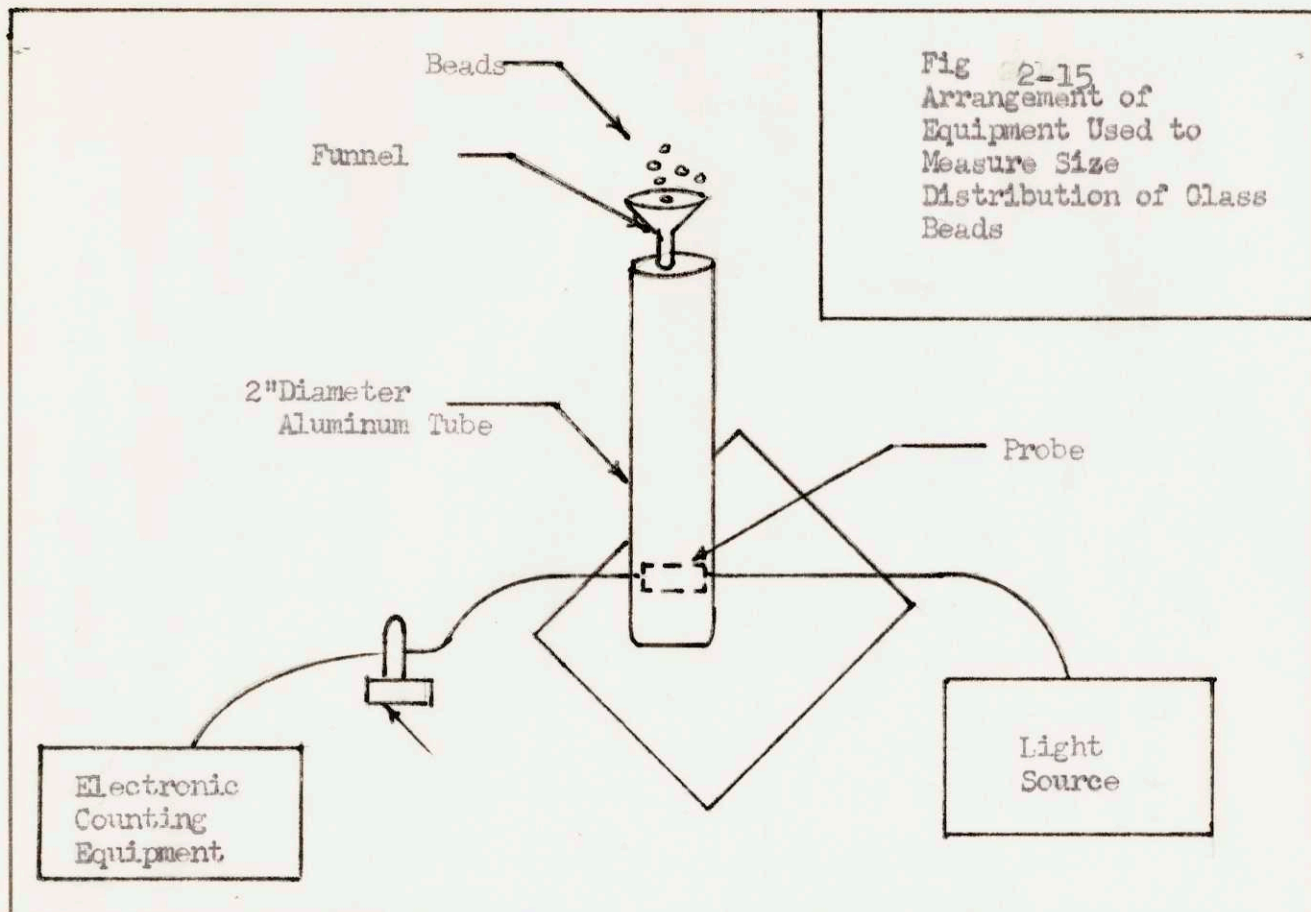
### Size Distribution Measurements

#### A. Glass Beads

Size distribution measurements of glass beads were made using the configuration shown in Fig. 2-15. The probe was inserted in the lower section of a 2" inner diameter aluminum pipe. During the experiment the beads were dropped through a funnel placed over the top opening of the pipe. They fell down the pipe, through the probe, and onto a paper placed under the open bottom end of the pipe.

After an initial warm-up period of one to two hours for the electronic equipment, the auto lamp was turned on and the constant D. C. level produced was recorded. This constant signal is referred to as the D. C. shift. Since high light intensities were striking the photo cathode continuously, photo multiplier fatigue resulted. Observations showed that the D. C. shift at the time the light source was turned on was 2500 mv, while after a period of ten minutes this D. C. shift diminished to 2000 mv. These fatigue effects required intermittent photo-tube rest periods during the experiments. Data taken at times of large variations in the D. C. shift were discarded.

After the preliminary set-up of the equipment and check of the electronics, data were recorded as the beads were gradually poured through the funnel. The oscilloscope time delay was set equal to the length of time for the slowest particle to



traverse the light field. All data was recorded by a 256 channel analyzer which kept a permanent tape record.

Care had to be taken to avoid any clogging of the probe by particles. Clogging would cause lower D.C. shifts since any particles stuck in the slit opening would reduce the light intensity reaching the receiver pipe. A test particle passing through an area blocked by a clogged particle would be erroneously measured. The occurrence of a few stuck particles would not hamper the final data, but large scale clogging would definitely invalidate the pulse height data obtained. Clogging can be easily corrected with air blown across the slit opening or air blown through the entrance hole for the receiver light pipe.

Data were taken with different probes and slit openings. The experimentally measured glass bead size distribution shown in Fig. 2-17 were taken with probe number 1. The D.C. shift was 2000 mv. The experimental distributions in Fig. 2-18 and Fig. 2-19 were taken with probe number 2. The height of the slit opening of the probe was varied by using three layers of Scotch Tape in the measurement of the distribution in Fig. 2-18 and two layers of tape in the measurement of the distribution in Fig. 2-19. In both cases the D.C. shift was 2500mv. The use of different probes with different light intensities was necessary in order to try to make the observed pulse height signal ( from a particle) to noise ratio as large as possible.

#### B. Water Spray from an Atomizer

The experimental set-up used for distribution measurements

of water droplets is shown in Fig. 2-16. The electronic arrangement was the same as that used in the glass bead measurements except for the shortening of the oscilloscope delay time to  $200\mu$  sec. so that multiple counts from the dense atomizer flow would not occur. This procedure of using a short delay time could lead to serious counting difficulties if the rise time of the observed pulse was below  $200\mu$  sec.; however, initial observations indicated a rise time of about  $100\mu$  sec. for most test droplets.

The apparatus was similar to that used for the beads except that no attempt was made to contain the particles in a cylinder. An air hose was placed next to the probe in order to direct the atomizer spray through the probe opening and to help prevent probe clogging. In this case the slit opening was made by using two pieces of Scotch Tape. The D. C. shift was 2000 mv. This distribution is shown in Fig. 2-20.

### C. Noise

Random noise data was taken by setting the oscilloscope trigger level low enough so that it fired on these pulses. A pulse height distribution is shown in Fig. 2-21.

### Experimental Results

The experimental results are shown in Fig. 2-18 to Fig. 2-24. Size distributions for the glass beads are given in Fig. 2-17 to Fig. 2-19. Fig. 2-20 shows the size distribution for the atomizer spray. Fig. 2-21 displays the noise spectrum caused by the constant high light intensity. Typical observed pulse shapes are shown in Fig. 2-22 and the effects of delay time on the observed spectra of colored water drops are shown in Fig. 2-20.

The top portions of Fig. 2-19 to Fig. 2-20 represent size distributions determined by the shadow technique. The ordinate of each graph represents the fraction of total counts falling between pulse height intervals. Since the diameter of each particle is proportional to the square root of the pulse height analyzer channel, the abscissa is plotted both as the square root of the pulse height analyzer channel and as particle diameter. In order to correlate the square root of channel number with particle diameter, the central point of the plateau in the top portion of Fig. 2-18 (a square root of channel number = 6) was set equal to the central point of the lower portion of Fig. 2-17 (a diameter of  $290\mu$ ). The relationships between the values of the listed diameters and square root of channel number for the top portions of Fig. 2-18 and Fig. 2-19 were obtained by relating the square root of channel number in each of these figures to that in Fig. 2-17 and using the previously determined ratio of size to square root of channel number. In relating the square root of channel number of Fig. 2-17 to that of Fig. 2-18 and Fig. 2-19 the effect of



different analyzer and light intensities used in the particle distribution measurements was taken into account. Since the opaqueness of the colored water drops differed from that of the glass beads, no diameter correlations with those in Fig. 2-17 was attempted. In this case the square root channel number of 10 was taken to correspond to  $57.5\mu$ .

The lower portions of Fig. 2-17 to Fig. 2-20 represent the distribution of particle size obtained by viewing the particles with a microscope. The ordinate of each graph represents the fraction of particles per diameter intervals while the abscissa represents the particle diameter.

Fig. 2-21 and Fig. 2-23 show the effect of oscilloscope delay time upon observed spectrum of photo tube noise and of colored water drops. The results are plotted as counts for a given pulse height versus pulse height analyzer channel number. The upper portion of each figure was taken when the oscilloscope's delay time was  $1000\mu$ sec. while the lower portion was taken when the delay time was  $500\mu$ sec.

Fig. 2-22 displays typical photo tube pulse shapes. These photos were taken as particle C passed the slit of probe number 1.

Fig. 2-17  
 Size Distribution  
 Measurements for Particle C  
 Type Glass Beads, Size  
 Range 400 - 200  $\mu$   
 Analyzer Range = 64 Channels  
 Gain = 1  
 D.C. Shift = 2000 mv.

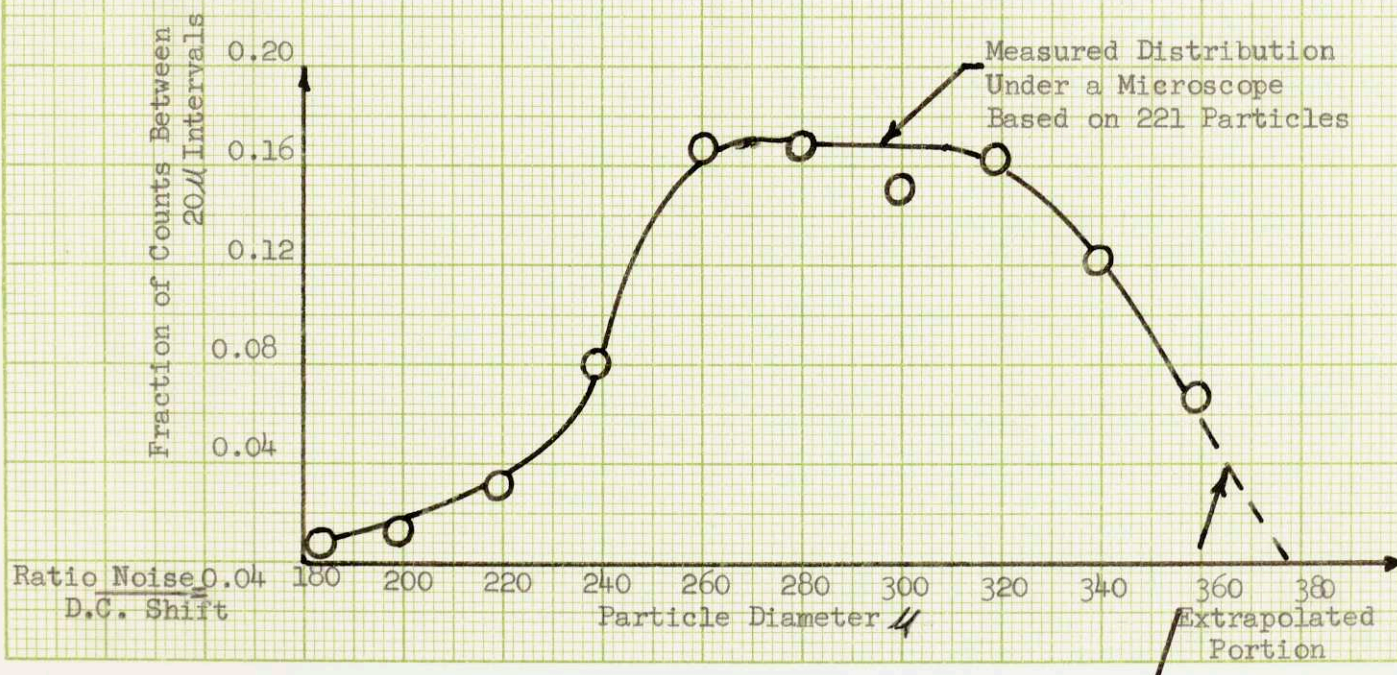


Fig. 2-18  
 Size Distribution  
 Measurements for Particle  
 H, Type Glass Beads, Size  
 Range 85 - 140  $\mu$   
 Analyzer Range = 256 Channels  
 Gain = 2  
 D.C. Shift = 2500 mv

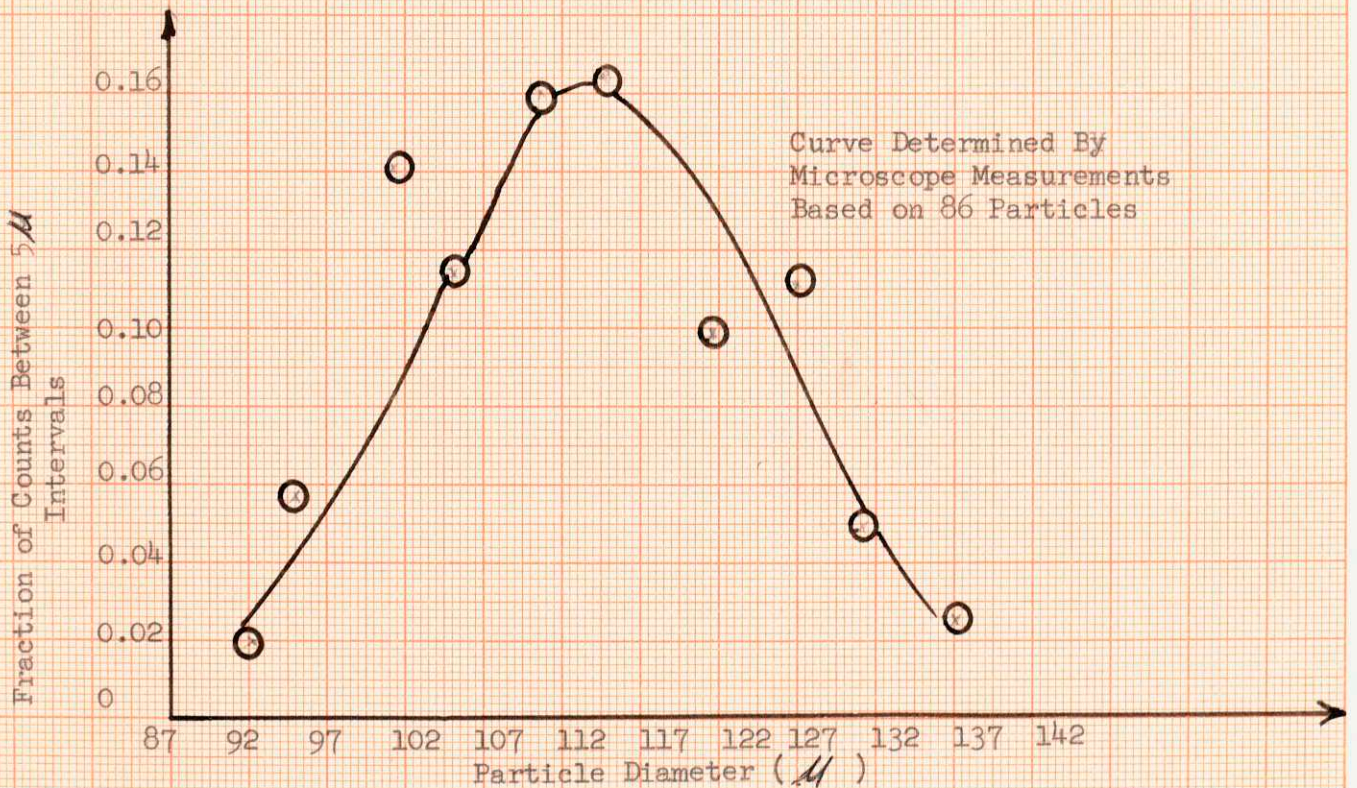
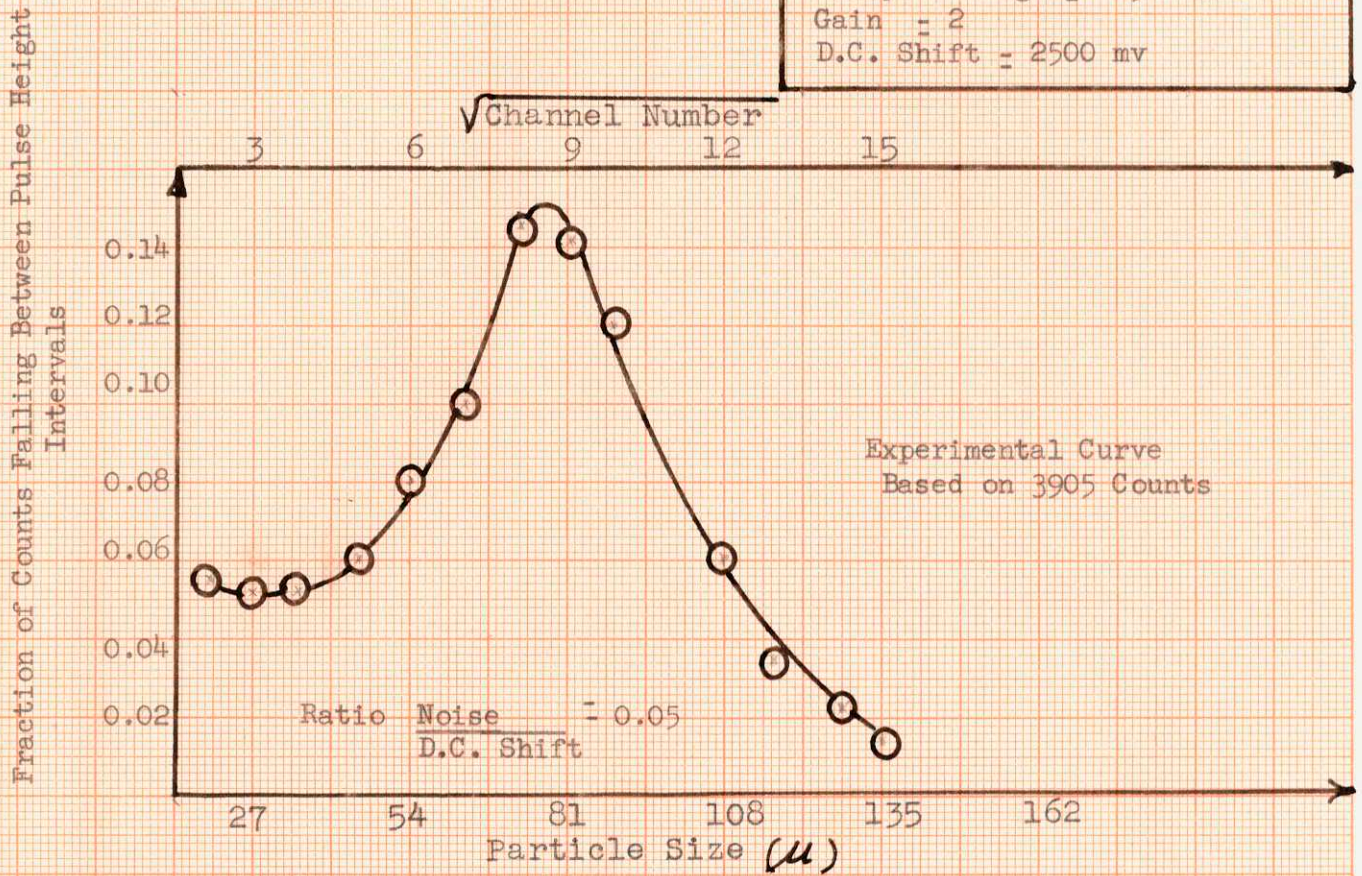


Fig. 2-19  
 Size Distribution Measurements for  
 Particle R, Type Glass Beads, Size  
 Range 60-10 $\mu$   
 Analyzer Range = 256 Channels  
 Gain = 2 D.C. Shift = 2500 mv

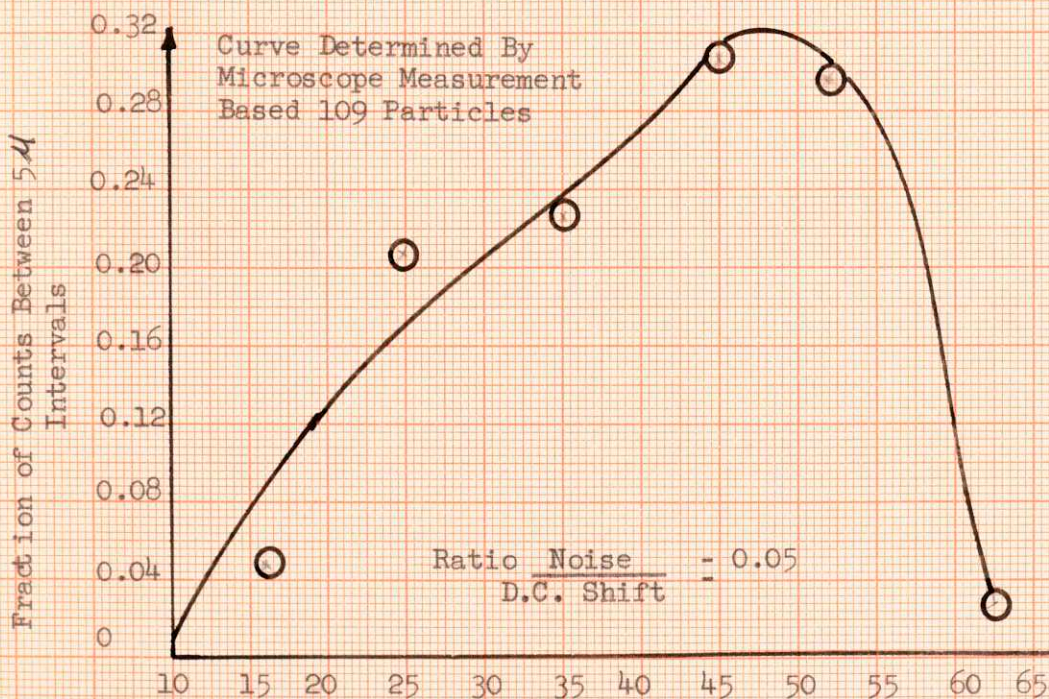
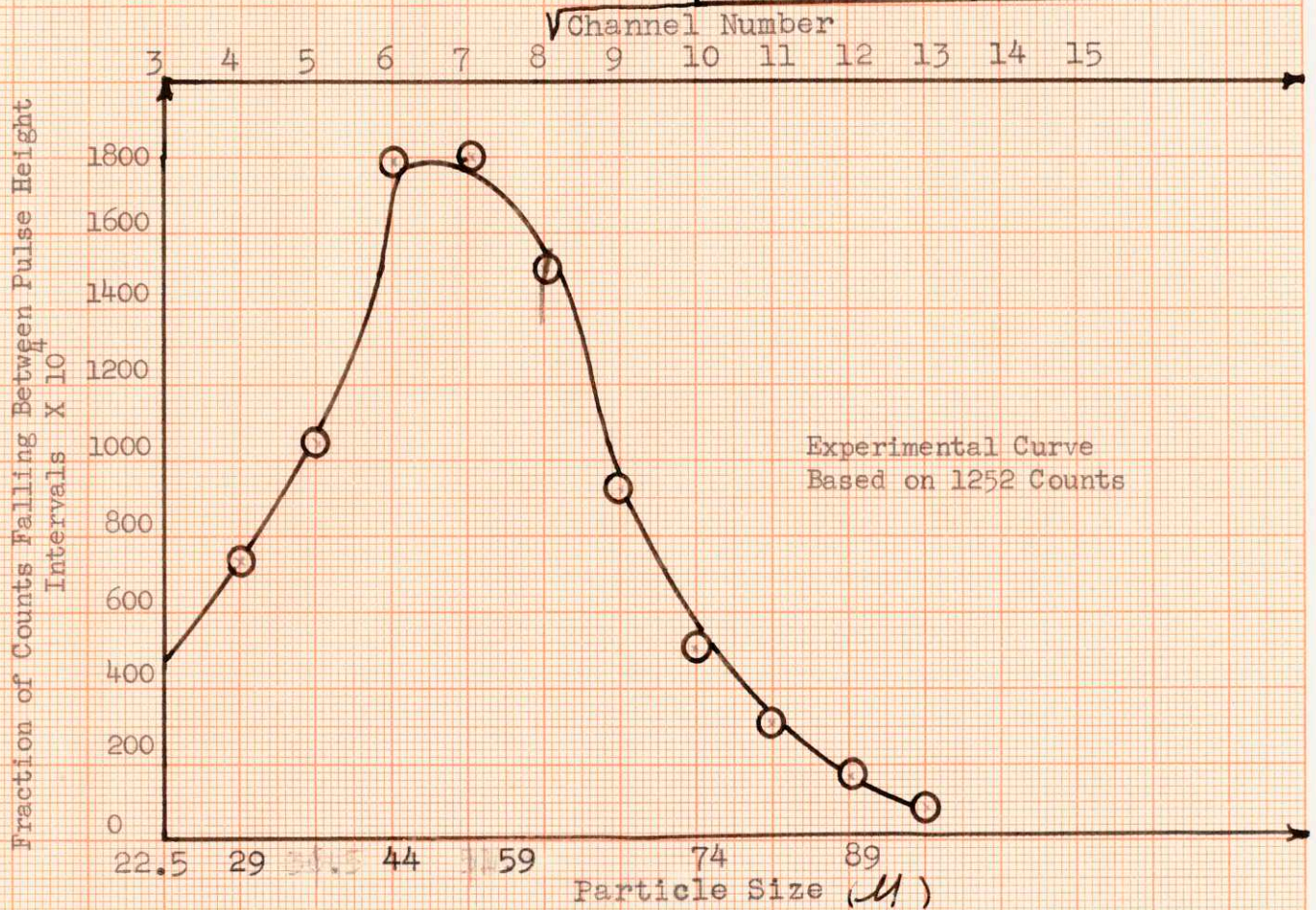
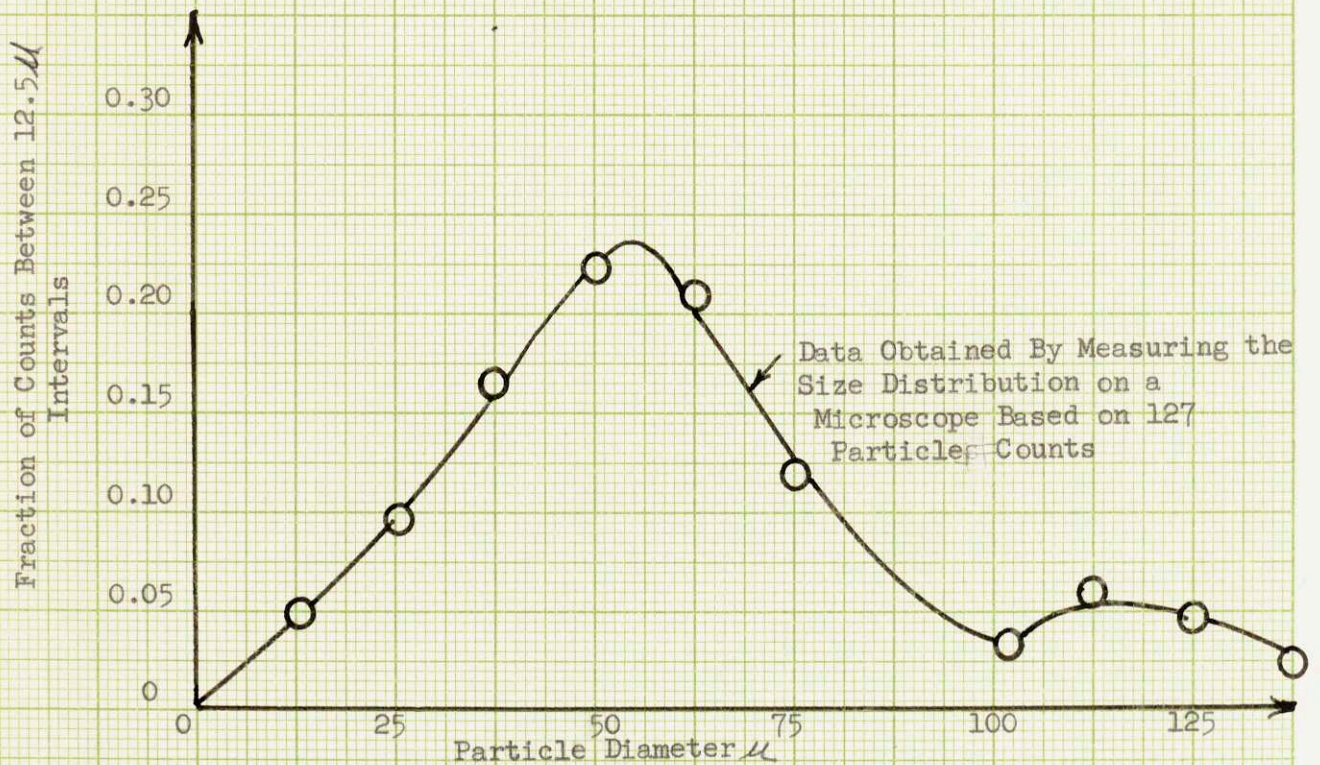
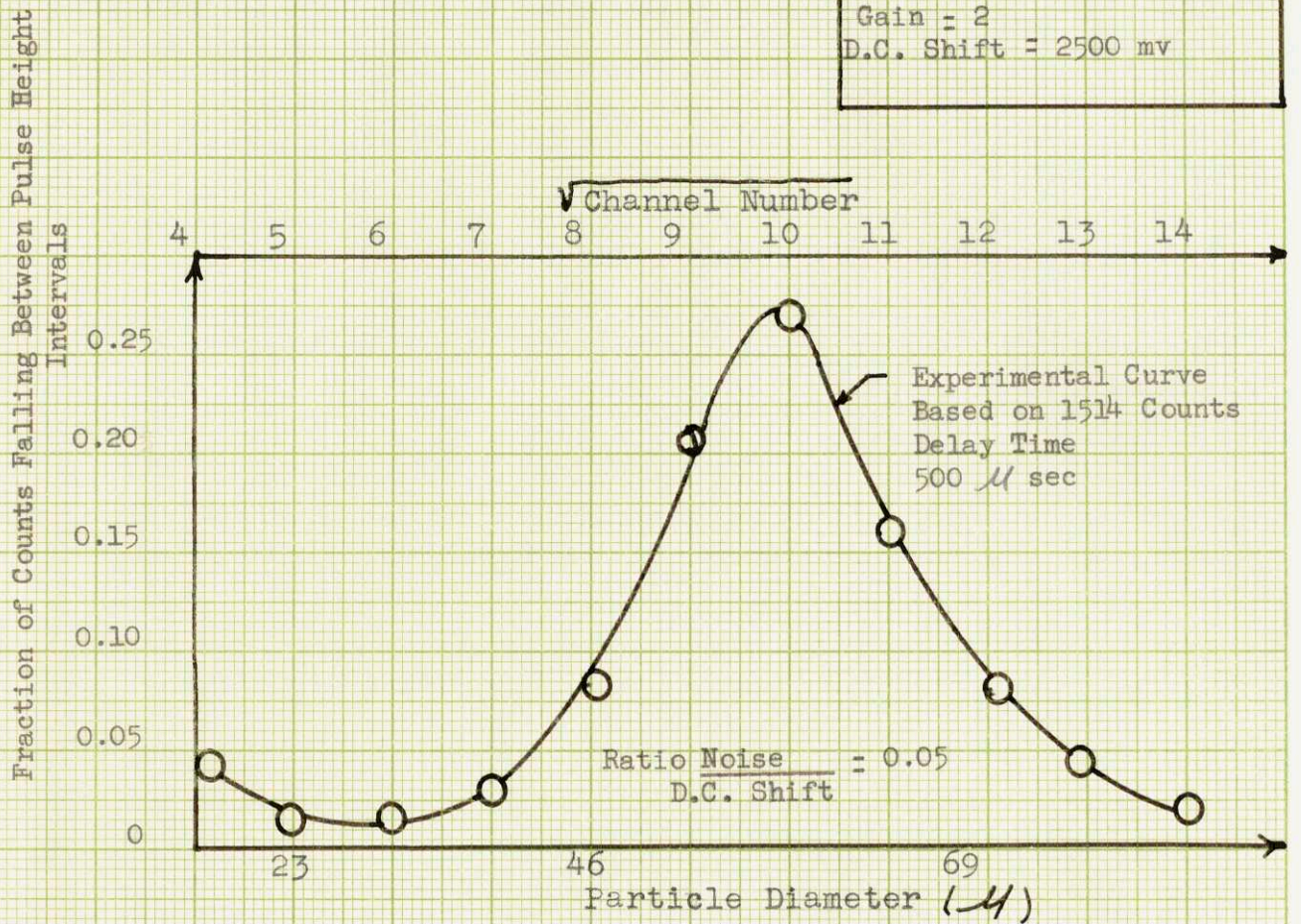
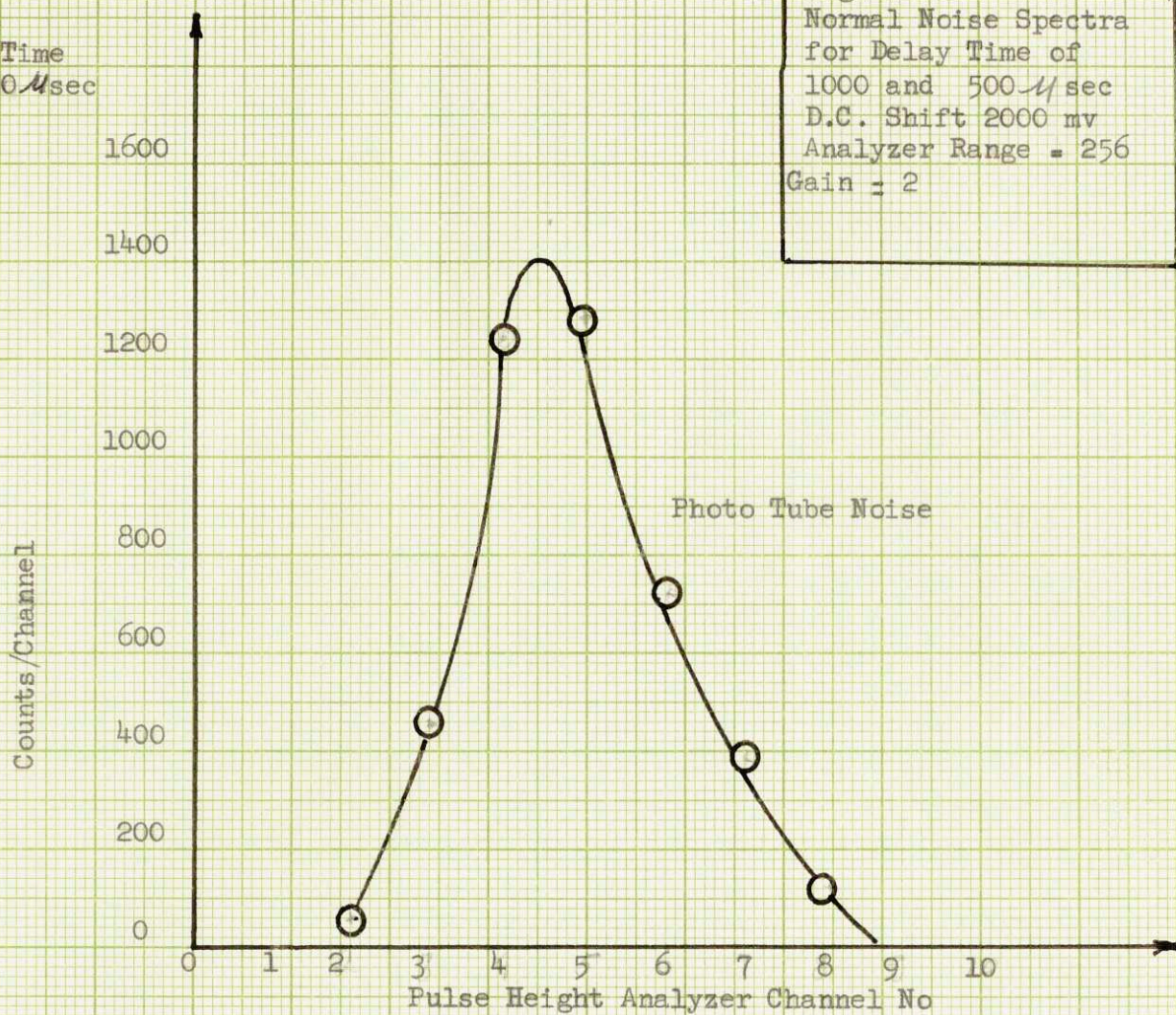


Fig. 2-20  
 Size Distribution of  
 Colored Water Spray  
 Analyzer Range = 256 Channels  
 Gain = 2  
 D.C. Shift = 2500 mv



a) Delay Time  
1000  $\mu$ sec



b) Delay Time  
500  $\mu$ sec

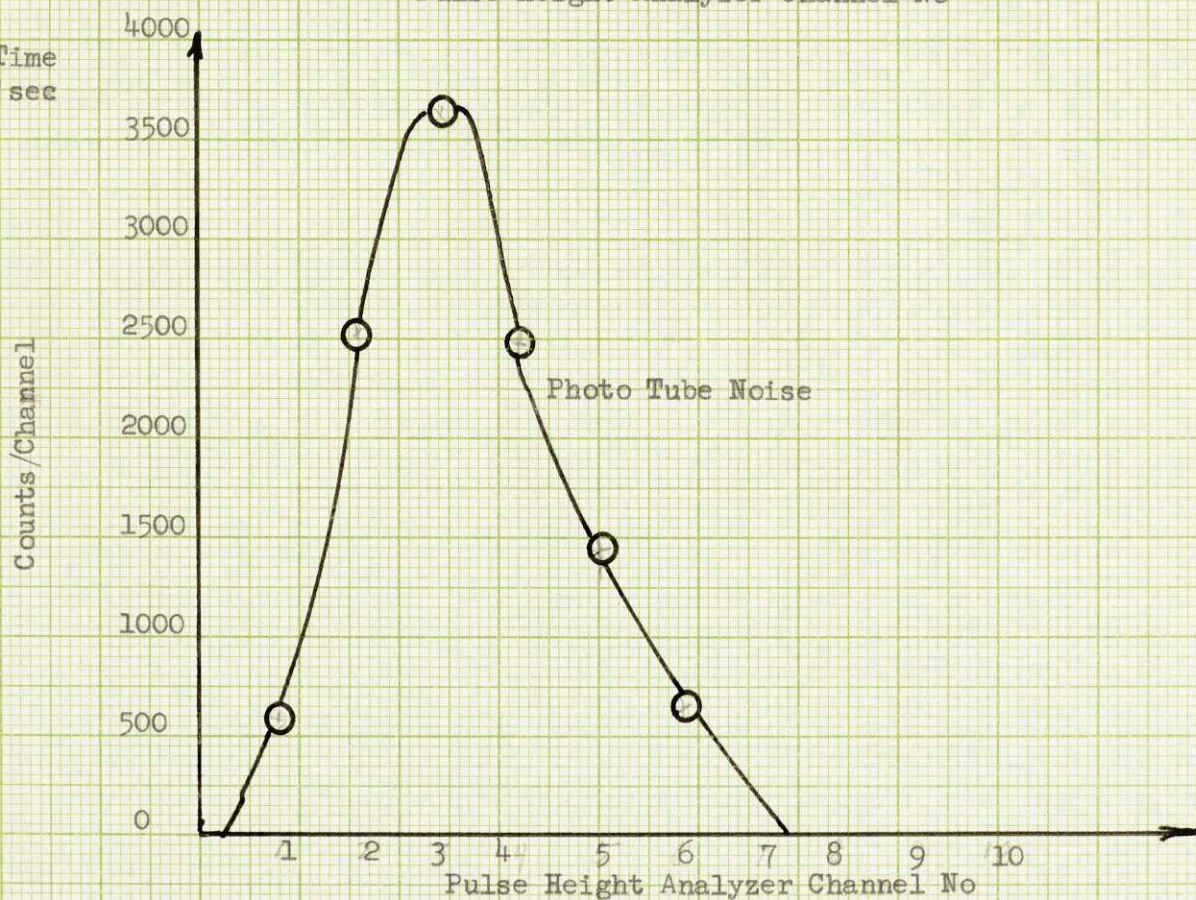


Fig. 2-22  
Photo of pulses for Particle C  
Passing Through Probe # 1

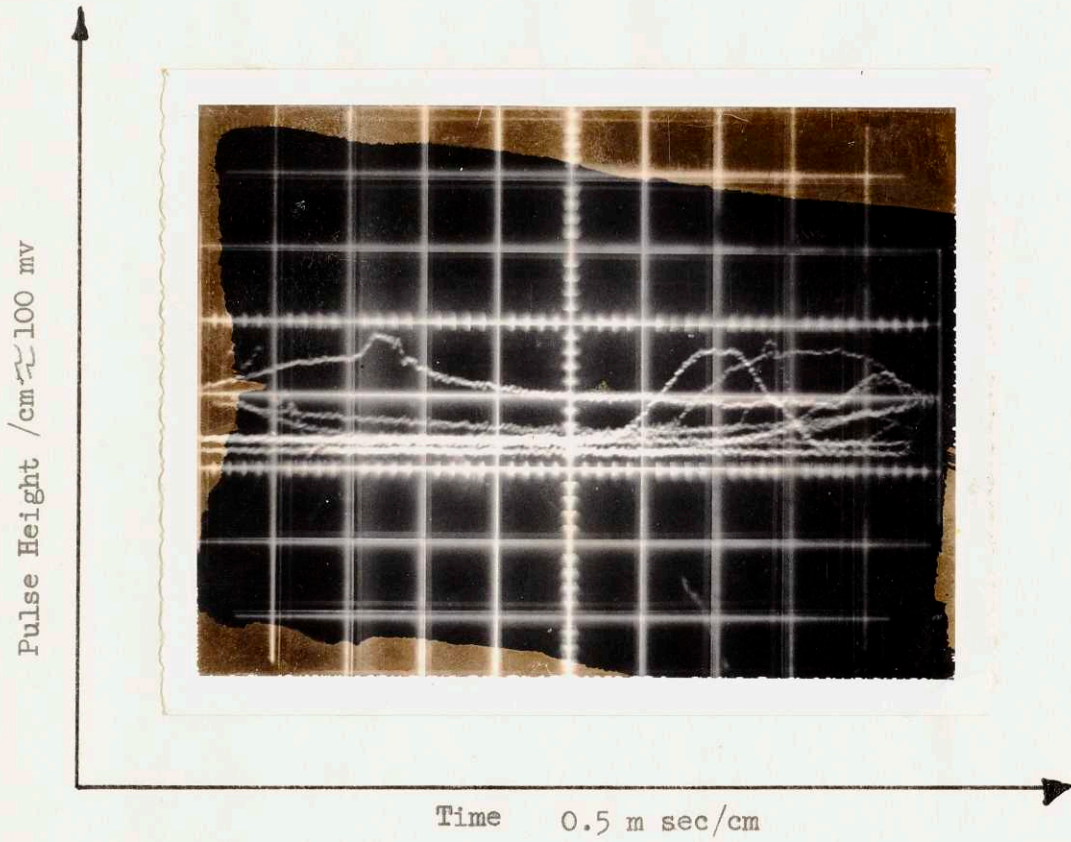
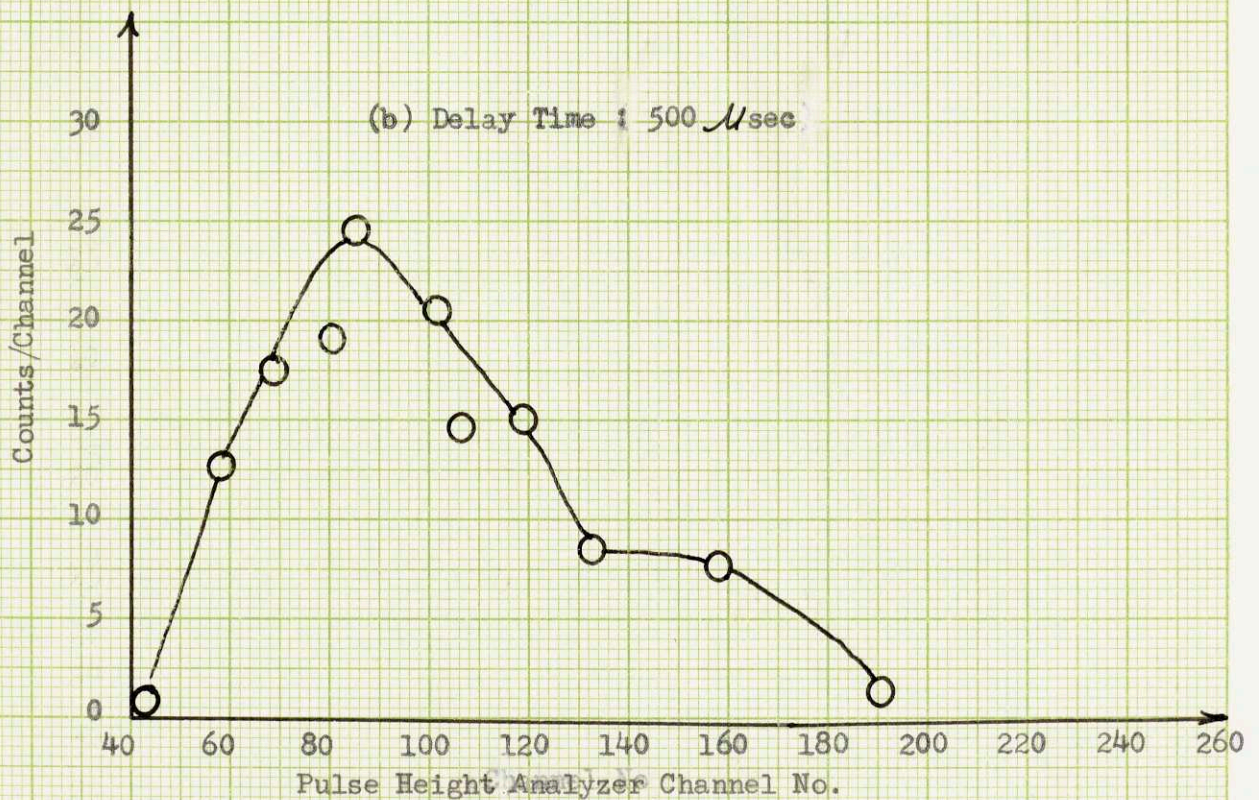
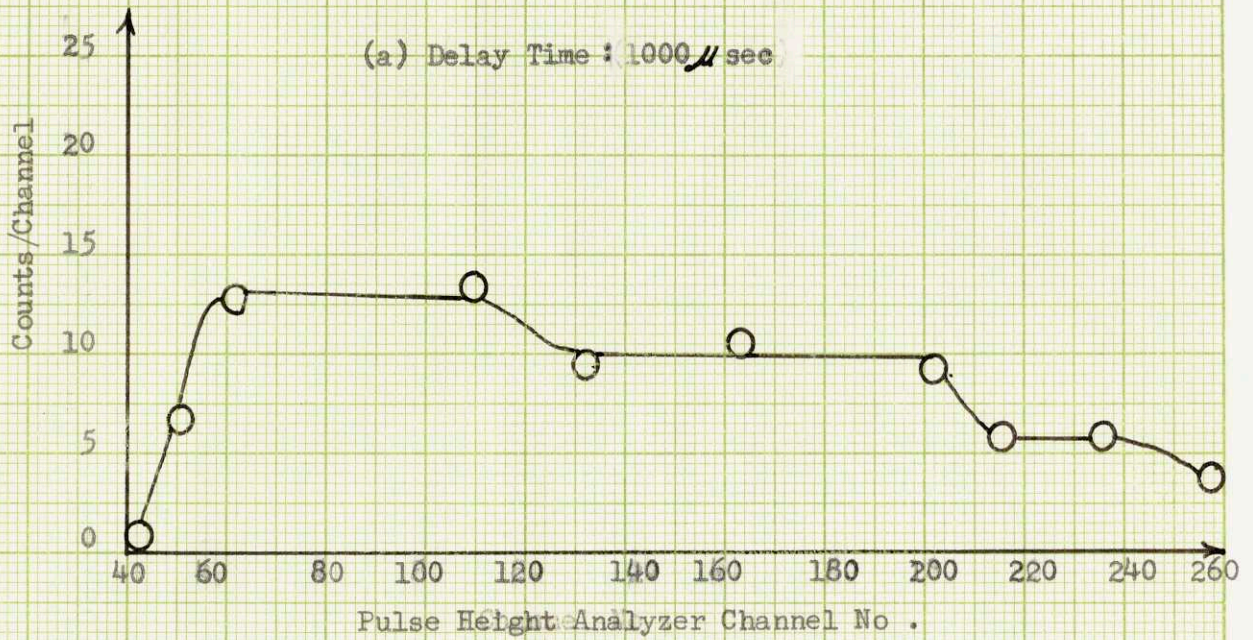


Fig 2-23  
 Spray Experiment  
 For Different Delay  
 Times Based on  
 3469 Counts

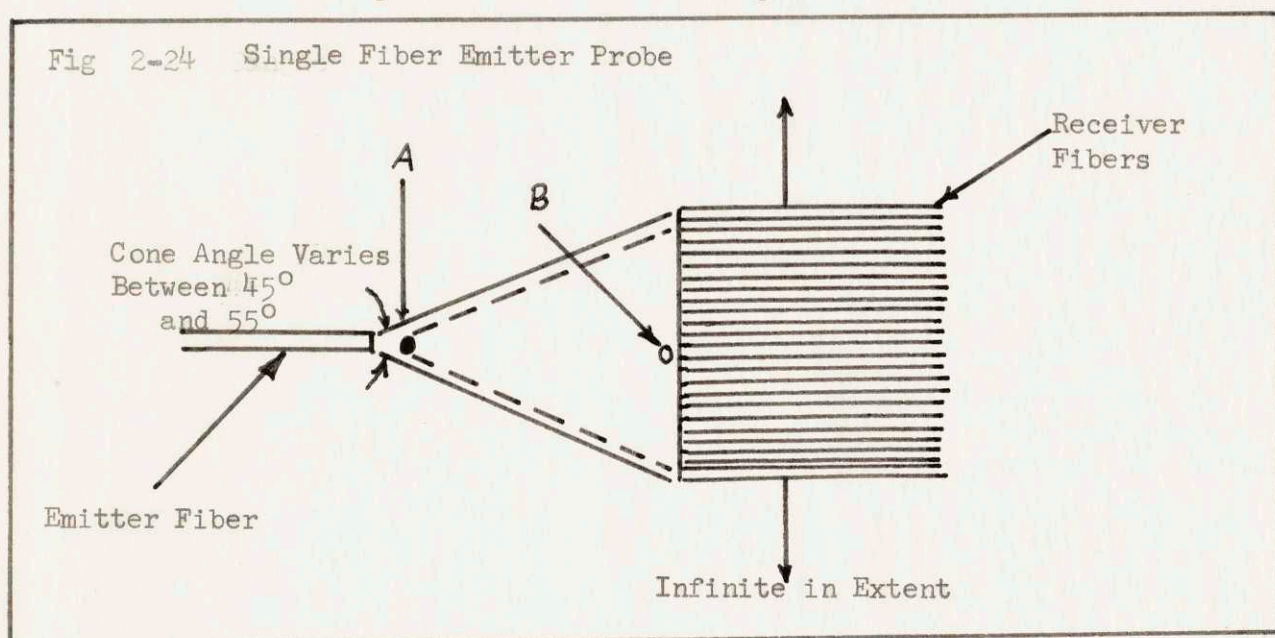




## DISCUSSION OF RESULTS

### A. Sources of Experimental Error

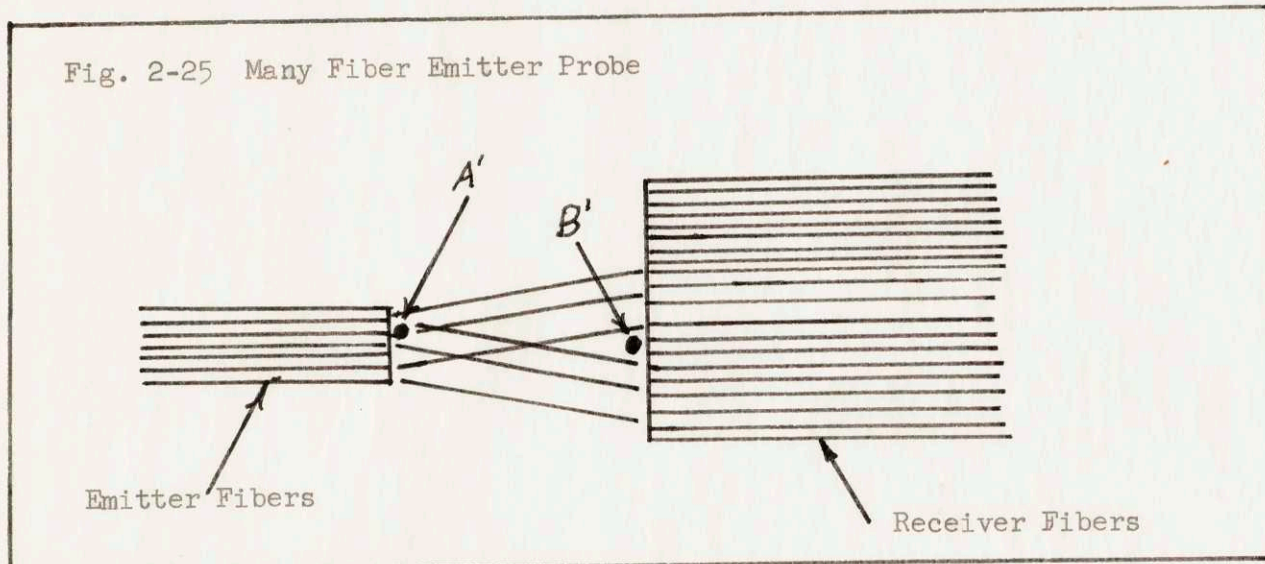
1) The emergent light beam from each fiber in the light pipe spreads into a cone of light with an angle between  $45^\circ$  and  $55^\circ$ . This discussion is aided by Fig. 2-24 which shows, in essence, a probe consisting of a single emitter fiber and an infinite number of receiver fibers. All particles placed in the light field are black and all diffraction phenomenon have been neglected.



Two particles of the same size are shown entering the probe at different positions A and B and at different times. From this figure, it can be noted that the particle at A intercepts a more intense light beam than its counterpart at B and hence absorbs more light. The size of the observed pulse will be greater at position A than at position B. Thus the size of the pulse observed depends upon the particles position in the light field.

When more than one emitter fiber is present the situation becomes more

difficult to analyze. Fig. 2-25 depicts this situation.



For a particle at position A' near the emitter probe the magnitude of the shadow cast on the receiver probe will depend strongly upon the light emitted by the few emitter fibers closest to the particle. While the magnitude of the shadow cast on the receiver pipe from those particles at B' will depend upon the light field emitted from many fibers. Without detailed calculations, it is difficult to predict at which position (i.e. A' or B') the particle will absorb more light. Attempts were made to reduce this effect by moving the emitter light pipe as far away as possible and by construction of a long narrow slit before the receiver pipe so that the rays of light entering the receiver pipe would tend to be more parallel.

2) The light spectrum emitted from a tungsten filament lamp depends upon the filament's temperature. Since the photo-tube's sensitivity is a function of wave length, any change in light spectra would produce a voltage change in the photo tube signal. Changes in light spectra could be due to varying filament voltages or the use of different type filament lamps in an experiment. Small voltage variations would

probably produce unnoticeable effects in light spectra, however, the spectral variation caused by the use of different type lamps can be larger and produce noticeable effects. Therefore the same lamp operating at the same voltage must be used when different experiments are to be compared.

3) Changing light intensity due to voltage variations in the battery charger. All D. C. power supplies have voltage variation in their output. The more expensive power supplies have in general less variations. Since a normal D. C. power supply was not available a battery charger connected in parallel to a 6 volt battery was employed. The magnitude of these variations were viewed on an oscilloscope and were found to have a height less than 1% of the output voltage. The effect of these voltages on the magnitude of the light field is not known, however these effects are assumed small since they were undetectable.

4) Bumps or surface irregularities on the glass beads would exhibit scattering properties different from the assumed spherical shape. In general, surface irregularities would cause more diffuse light scattering than perfectly spherical particles. Close examination of these beads showed no appreciable irregularities present.

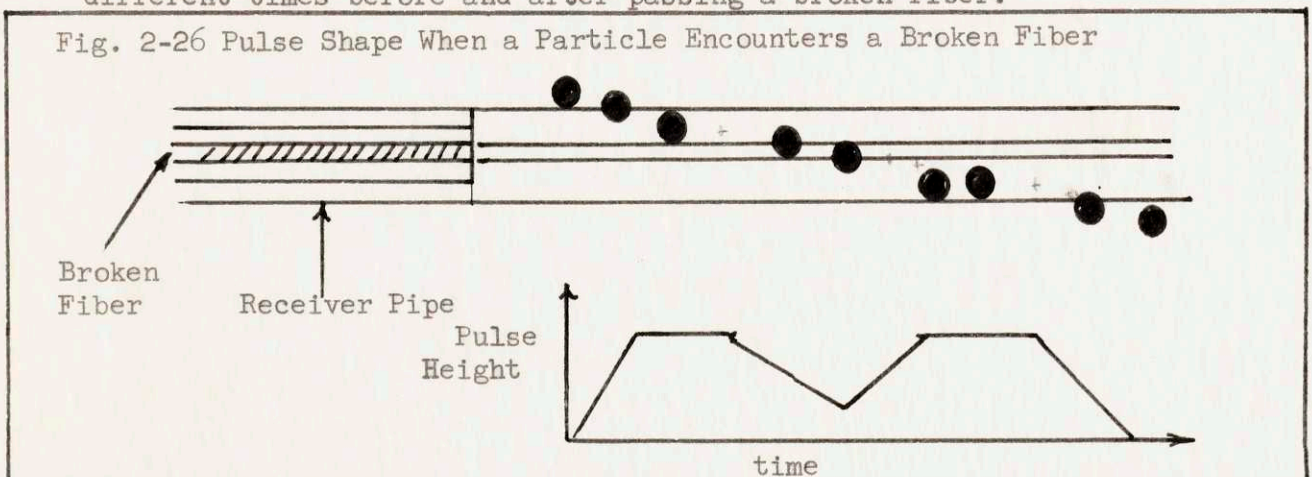
5) Probe Clogging is caused by water droplets or glass beads becoming lodged in the narrow slit opening of the probe. Clogging of the slit by only a few test particles would not hamper significantly the detection procedure. However, the collection of a large number of particles will reduce the light intensity reaching the test particle. The test particle would intercept less light than in an unhindered light beam

and a lower output pulse would result. The magnitude of this effect is analyzed analytically. The best procedure is to try to avoid clogging by constantly measuring the D. C. shift and discarding any suspicious data. This procedure is not foolproof and the effects of clogging were present to some degree. The magnitude of these effects is not known but should be small.

6) At least 10% of all the fibers in each light pipe had been broken. These breaks were caused by bending the fibers at sharp angles.

In the case of small particles and thick slit openings, this effect on the maximum height of the observed pulse is small. However in the case of slits of the order of two to three fibers thick and particles of the same size or greater than the diameters of the fibers, the presence of these broken fibers can seriously affect the observed maximum pulse height.

The pulse distortion depends upon the broken fibers position in the probe. In general if the pulses reach their maximum value obtainable in an unbroken fiber probe before or after their encounter with a broken fiber, the observed pulse height spectrum will not be affected. This can happen only if the probe is thick enough and the particle small enough so that the pulse may build up and reach the flat portion of the pulse shape. Fig. 2-26 is a cross sectional view showing a small particle at different times before and after passing a broken fiber.



If the probe is narrow, it is very likely that a broken fiber will be encountered before the pulse has reached its constant value. Moreover, there are not enough fibers present after this encounter to enable the pulse to recover and reach its maximum. In essence the result is a lower observed pulse height value than if no broken fibers were encountered. Again an analytic solution is impossible.

The fraction of particles which encounter a broken fiber may be of interest. The following analysis is a very rough calculation procedure of this quantity which may be incorrect by a factor of two. Eq. 3 represents this fraction. This equation is based on a slit containing 75  $\mu$  fibers, m fibers thick and n fibers wide with 10% broken fibers. The diameter of the test particle is d. Assuming a uniform distribution of broken fibers yields eq. 3

$$f = m(0.1 \times n \times 75 \text{ } d) / n 75 \quad (3)$$

where f = the approximate fraction affected

d = average diameter of test particle

This fraction has been evaluated for the cases encountered experimentally, and is found in Table 2-2

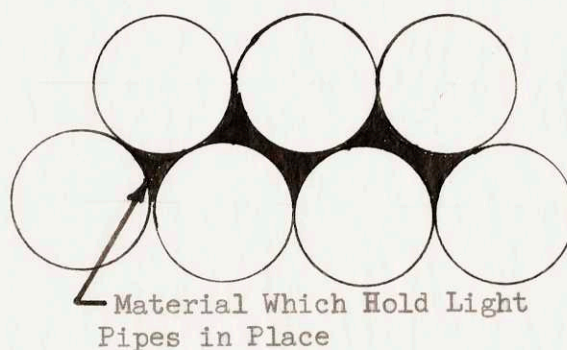
Table (2-2) Fraction of Particles Affected By Broken Fibers

<u>Particle Identification Group</u>	<u>f</u>
C	all
H	0.5
R	0.16
Spray	0.2

From these calculations it can be concluded that these broken fibers affect a large fraction of the data.

7) The light pipes' fibers have a finite diameter and form a configuration such as that shown in Fig. 2-27.

Fig. 2-27 Details of End Surfaces of Light Pipes

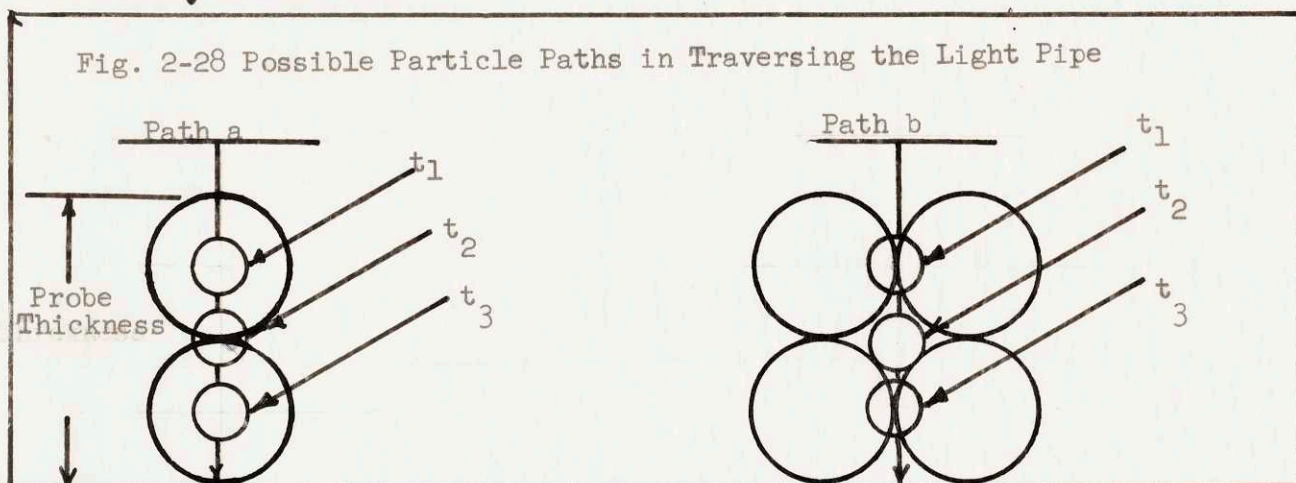


Since the pipes have a circular cross section they contact each other at a few points only. In the space between each pipe is placed a cement which bonds the pipes together. The frontal area of this cement is small in comparison with the frontal area of the light receiving surfaces. For thick probes and particles larger than the average diameter of the fiber, this small variation of the light receiving surface should not affect the pulse height very much. A rough estimate of the average inaccuracy due to these effects is that the decrease in pulse height is equal to the ratio of the inactive area to the total probe area. Based on a square slit completely filled with circles this decrease is 23%. In the case of large test particles and a thick probe all the data (recorded pulse height distribution) should be uniformly affected so that the pulses on the average are 77% of their true value. However, the shape of the distribution

is not changed.

For the data taken, only those of particle identification group C fall in the above class. The probe was  $400\mu$  thick or 5 fiber diameters (fiber diam  $\approx 75\mu$ ) and the smallest particle sizes were approximately  $225\mu$  or 3 fiber diameters. The data taken on particle H and the subsequent smaller particles is affected by these dark areas because fairly narrow probes (about 1 or 2 fiber diameters) and small particles were used.









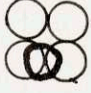

The particles' path through the light field and the position of the receiver light pipe influence the height of the observed pulse. For example, consider Fig. 2-28 which shows a given size particle as it passes the light fibers at different times of its descent. Two alternative paths a and b are considered.



Considering path a it is noted that the maximum pulse height is observed at times  $t_1$  and  $t_3$ . The minimum pulse height is observed at  $t_2$ . Since the decrease in light intensity at times  $t_1$  and  $t_3$  is the maximum possible, under any conditions, the observed spectrum of pulses when path a is employed will not be distorted. If path b is chosen the maximum shadow cast at time  $t_1$  and  $t_3$  will be reduced by the dark cement spots. The observed pulse heights will be some fraction of the observed pulse height spectrum of a particle

traveling path a . Since the observed pulse height depends upon the particles path through the light field, the final pulse distributions will be different than that of the test particles' distribution. An exact analytic discussion of this problem is difficult. The following table lists the fractional decrease in light intensity for given particle, size and position.

Table 2-3 Fractional Light Intensity Decrease

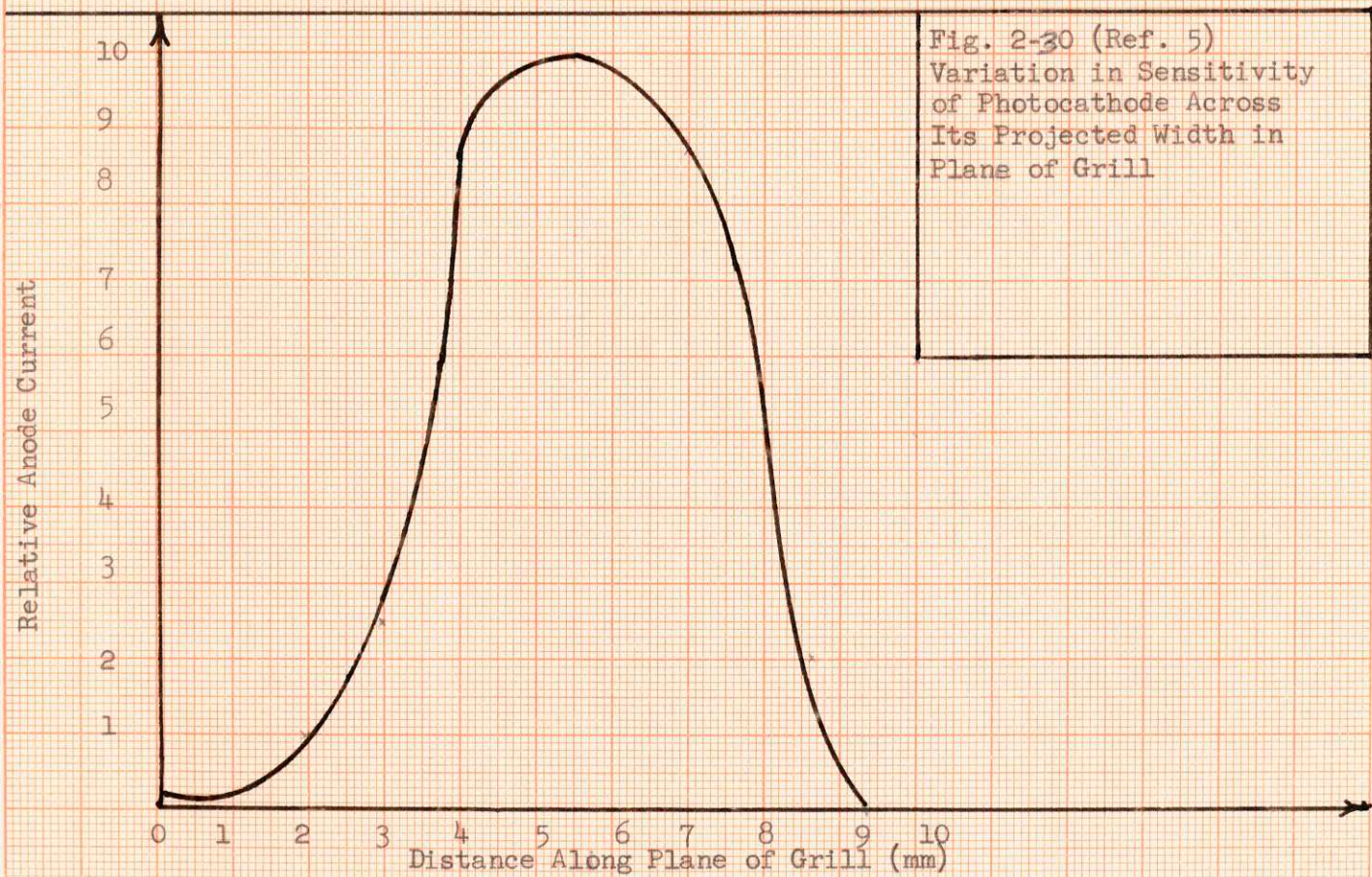
<u>Particle Group</u>	<u>Position</u>	<u>% Decrease</u>
C	Any	23%
H		23%
H		15%
H		23%
H		27%
R		91%
R		10%
R		0%
Spray		57%
Spray		17%
Spray		0%



8) The sensitivity of the photo cathode varies with vertical and horizontal position (see figures 2-29 and 2-30). In general the light beam emitted from each light fiber will have a cone angle spread between  $45^{\circ}$  and  $55^{\circ}$ . This cone of light will strike the photo-cathode with a radius of approximately 0.5 cm. If we assume that the center of the light fiber is pointing at the most sensitive point on the photo-cathode a sensitivity varying from 100 (arbitrary units) to 92 may be expected in the vertical direction and a sensitivity varying from 100 to 0 may be expected in the horizontal direction. In other vertical locations the variation over 1cm length can be from 99 to 6. Since the light pipes are small, and hence the light fibers are near each other they project light on almost the same circle on the photo-cathode. Although the photo-cathode sensitivity variation across an individual circle can be large, all fibers have roughly the same value for this variation. Therefore, these effects produced little nonlinearity. It should be noted that care must be taken in all experiments to have the light pipes remain in a constant horizontal position, if consistent experimental results are expected.

9) Burn out of the photo-cathode could result from over-exposing certain localized portions of its surface to a high intensity constant light flux. This high intensity light flux depletes the light sensitive phosphorus on the photo-cathode surface. As a result of this a decreased sensitivity will be encountered over the course of several experimental runs.

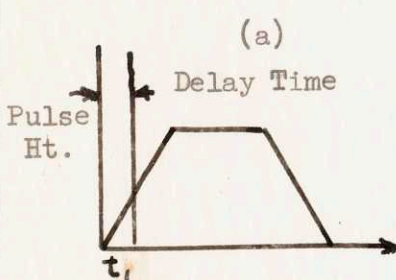
10) The signal conditioner has a time constant of approximately



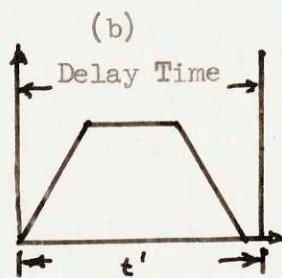
30  $\mu$ sec. for incoming pulses. The pulse length should be 4 or more times this value for accurate pulse height reproduction. Shorter pulses will not have sufficient time to build-up to their maximum value. These pulses will produce poor data. The minimum pulses encountered which resulted from fast water drops were above 200  $\mu$ sec. therefore the data was not degraded by this effect.

11) The delay time of the oscilloscope is the total time available for pulse counting. For best results the delay time should be slightly longer than the time required for the slowest particle to pass the probe. Too short a delay time may result in clipping the observed pulse before the maximum value of the pulse height has been reached. Fig. 2-31 is a summary of these effects.

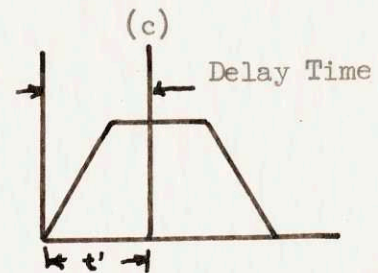
Fig. 2-31 The Delay Time Effect



Note:  $t_1$  is too short the pulse height maximum has not been reached.



Note:  $t'$  (the delay time) is longer than the pulse and the entire pulse can be counted.



Note:  $t'$  (the delay time) is shorter than the pulse length, however the maximum value of the pulse has already been obtained and no incorrect pulse height will be recorded.

A delay time which is too long can be harmful in dense flows. If two particles pass the probe at the same time, it is impossible to distinguish between them. However, if two particles enter at different times and the time between their entrance into the probe is less than the delay time only the larger particle will be observed. This result is due to the capacitors ability to store only the maximum recorded voltage for events happening during a single counting period (or delay time).

In the glass bead experiments the fraction of counts missed may be estimated by treating the delay time similar to a dead time. The fraction of counts missed may be estimated by eq. 2-2, if the pulses are assumed to occur at random time intervals and the possibility of two particles simultaneously entering the probe is neglected.

$$f_m \approx \left( \frac{1}{1-n\tau} - 1 \right) \quad (2-2)$$

where  $n$  = number of counts/sec.

$f_m$  = fraction of particles not counted

$\tau$  = the delay time

The following table lists this fraction for the various data collected:

Particle	Delay Time ( $\mu$ sec)	Approx. $n$ Counting Rate (in counts/sec.)	$n\tau$	$f$ missed
C	5000	20	0.10	0.11
H	5000	20	0.10	0.11
R	1000	30	0.03	0.03
Spray	500	200	0.10	0.11

In case of the spray the delay time had to be reduced so that this effect of missing counts was not noticeable. Fig. 2-23 shows the observed spectrum recorded for longer delay times. Note that the observed spectrum is peaked at a higher value from those spectra obtained with a slower delay time. The consistent trend of the peak value of this data to higher pulse height values in Fig 2-23 (lower) shows that only the larger pulse of a group of pulses entering the probe within a delay time was recorded. Table 2-5 lists the fraction of counts affected in this case.

Table 2-5 Fraction of Counts Missed for Data Displayed in Figure 2-25

<u>Curve</u>	<u><math>\tau</math>(<math>\mu</math>sec)</u>	<u><math>n</math>(particles/sec)</u>	<u><math>n\tau</math></u>	<u><math>f_m</math></u>
Fig. 2-25 upper	1000	200	0.2	0.25
Fig. 2-25 lower	500	200	0.1	0.11

12) Three types of photo tube noises were encountered. These were 1) noise resulting from the spontaneous emission of electrons on the photo-cathode, 2) noise in the steady D. C. voltage resulting from the high light intensity incident upon the photo-cathode surface, and 3) unknown origin noise.

The noise produced by spontaneous electron emission from the photo-cathode has a low pulse height magnitude (about 2-4 mv) when compared to the high value (about 100 mv) of the photo multiplier output noise due to large anode currents. Because of these low pulse height values, the occurrence of this noise may be neglected.

The photo tube output noise resulting from a high intensity light

beam striking varied between 2.5 % and 5% of the total constant D. C. voltage output. Most of the noise appeared to be in the frequency band  $10^3$  cps to  $10^4$  cps although the entire frequency spectrum of noise covered many more bands.

The magnitude of the noise signal determines the minimum particle size that can be accurately analyzed. In general pulses of the same order of magnitude as the noise pulses are difficult to analyze. The maximum expected pulse height from a given particle is the area of the particle divided by the total slit area multiplied by the total constant D. C. shift in voltage when no particle is in the light field. Table 2-6 lists the predicted ratio of maximum particle pulse height to the constant D. C. voltage output and the experimental ratio of noise pulse height to constant D. C. voltage output for the distribution measured in Fig. 2-18 to Fig. 2-21. The predicted values were based on the average particle size in each distribution.

Table 2-6 Ratio of Expected Particle Pulse Height to D. C. Shift Pulse Height

<u>Particle Group</u>	<u>Max. Predicted Ratio</u> <u>Pulse height</u> <u>D. C. shift</u>	<u>Expt. Noise Ratio</u> <u>noise height</u> <u>D. C. shift</u>
C	0.15	0.04
H	0.06	0.05
R	0.01	0.05
Spray	0.03	0.05

The effects produced on the observed pulse height distribution due to these noise pulses are difficult to determine. The noise effects can increase or decrease the size of the observed pulses. An analytic

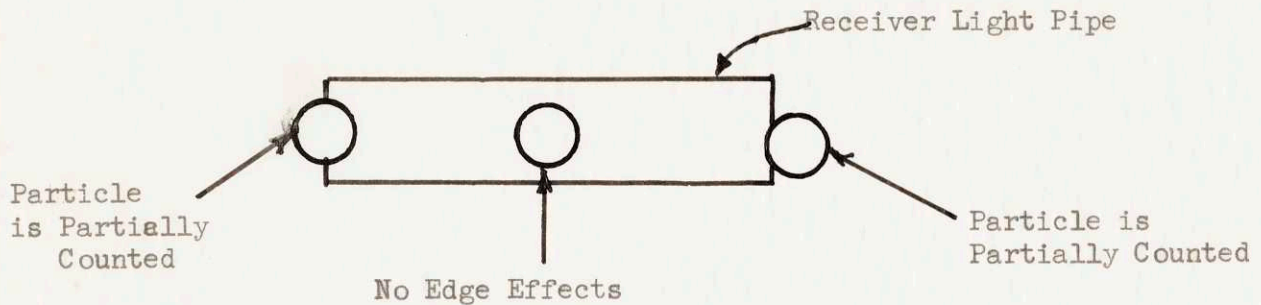
solution of the noise problem requires knowledge of the noise frequency spectrum, the time occurrence of the pulses and the period and shape of the expected pulses. Since these parameters could not be determined with available equipment, these noise effects could not be evaluated. Qualitatively one might say that when the noise pulses are much lower than the particle pulse height, the noise effects are small. Only in the measurement of the distribution of particle C was the value low enough so that a particle distribution could be measured.

Fig. 2-21 displays the observed pulse height distribution of noise. The data for this figure was obtained by using the experimental set-up shown in Fig. 2-12 with the triggering level of the oscilloscope adjusted so that it triggered on noise pulses. The delay time of the oscilloscope was varied to determine whether trends in the observed data could be predicted. More low noise pulses were observed with a decrease in delay time. This is due to the fact that the signal conditioner will recognize only the largest pulse it observes within a counting time equal to the oscilloscope delay time. During a long delay time several pulses will enter the signal conditioner and only the largest will be recorded. For shorter delay times fewer pulses will enter and the resulting distribution will show more smaller pulses. The distributions will be better approximated when shorter delay times are used. Fig. 2-23 (upper and lower) shows a gradual shift to lower pulse height values as the delay time is reduced from  $1000\mu\text{sec.}$  to  $500\mu\text{sec.}$

In summary, the manner in which noise variations influence the observed data has not been determined.

13) Edge effects are caused by particles partially entering the light field with the result that only part of their shadow is cast on the receiver pipe. The observed pulse height spectrum is lower than that which would be expected if the entire particle entered the light field. The occurrence of these edge effects is shown in Fig. 2-32, which shows 3 particles vertically descending past the slit. Edge effects are prevalent in two of these.

Fig. 2-32 Examples of Edge Effects



An analytic determination of the manner in which this effect influences the data is difficult. The number of particles affected may be approximated and form a basis for qualitatively looking at data. Assuming that a particle's probability of being inside or slightly outside of the light field is constant, the fraction (see eq. 2-3) of particles affected is approximately the ratio of twice the particle diameter to the sum of the length of the slit and twice the particle diameter.

$$f^l = \frac{2d}{L + 2d} \quad (2-3)$$

$f^l$  = the fraction of particles affected by edge effects



where  $d$  = the diameter of particle

$l$  = length of slit

This fraction is tabulated in Table 2-7 for the average measured diameter of particle size observed under a microscope.

Table 2-7 Fraction of Particles Affected By Edge Effects

<u>Particle Group</u>	<u>Av. Size (<math>\mu</math>)</u>	<u>Length of Slit (<math>\mu</math>)</u>	<u><math>f^1</math></u>
C	280	1000	0.35
H	118	1000	0.19
R	35	1000	0.07
Spray	57.5	1000	0.10

## B. Discussion of Measured Spectra and Observed Pulse Shapes

Fig. 2-22 displays some of the observed pulse shapes. These photos were taken at the input of the signal conditioner. Most of the discernible pulses show exactly the same characteristic rise, flat, and fall sections as the ideal pulse shown in Fig. 2-2. Hence it may be concluded that the reasoning which led to Fig. 2-2 is correct and that all parts of the system up to the oscilloscope are functioning properly.

The top portion of Fig. 2-17 shows the experimental measured size distribution of particle C while the bottom section shows the size distribution as measured by a microscope. Comparison of these distributions is based on the observed shape. Both distribution have distinct rise and fall sections, and a flat top section. The absolute value of the slopes is higher for the left slope than for the right slope in both measurements. The top portion of Fig. 2-17 may be lowered by noting that the ordinate values considered points only between ( $\sqrt{\text{chan, no. 4 \& 8}}$ ) while that in the lower portion considers points almost over its entire range of values. If the extrapolated portions of the experimental curve are considered in computing the value of each ordinate point, these points will be reduced by  $\frac{\text{area between } \sqrt{\text{channel no. 4 \& 8}}}{\text{Total Area}}$  which is approximately 0.815. This will effectively shorten the height of the experimental curve and make it look more like the measured curve. Another quantity of interest is the range of diameter covered by the flat plateau. The experimental curve yields  $(7/5=1.4)$  1.4 while the measured (lower curve) yields  $(320/258=1.25)$

1.25. These values are in close agreement. The ratio of diameters encountered when the ordinate's value is equal to  $\frac{1}{2}$  the maximum peak value is 1.5 for the measured curve and 2.2 for the experimental curve. These values state that the experimental curve is broader.

Table 2-8 lists the major non-linear factors found in the first part of this discussion. As seen in this table about 35% of the particles encounter the Edge Effect. Since only portions of the particle are observed, this effect will tend to broaden the left side of the experimental curve.

Table 2-8 Major Non-Linear Factors

Particle	C	H	R	Spray
Edge Effect f=	0.35	0.19	0.07	0.10
Ratio <u>Pulse ht</u> noise	3.5	1.2	0.2	0.6
Time delay f	0.11	0.11	0.13	0.11
Broken fibers f	1	0.5	0.16	0.2
Finite size of light pipe(fraction which may be missed)	23% constant	15-27%	0-91%	0-5%

f stands for the fraction of particles affected.

The noise pulses can broaden the observed spectrum. As depicted in Fig. 2-21 (upper) these pulses ranged from a channel number of 0 to 9 with the average about 4. The observed spectrum ranged from channel number 16 to 64. The addition or subtraction of these noise pulses to the particle pulses produces a broadening effect upon the measured distribution. The effect of this distortion upon the measured distribution of the larger sized particles (those that produced

pulses in channel number 50) would not be as great as that upon the smaller size particles ( those that produced pulses in channel no. 20). Since a quantitative estimate of the edge effect and the noise effect could not be made, differences between the observed and measured spectra can not be attributed to just these two effects.

The number of particles used to determine the measured curve is only 221, and points on the plateau contain between 30 and 40 particles. If we assume a normal distribution for each point then the number of particles per point would have a standard deviation whose value is about 16% of the number of particles per point. Points forming the slopes would have an even greater percentage standard deviation. Statistically the experimental curve is better since it contains more data samples than the microscope measured curve. Based on the general shape of the two curves, the factors which tend to make the experimental curve broader, and the small number of measured points, the agreement between the two curves is good. Moreover the data obtained using particle C can be expected to be useful since the signal to noise ratio, the main contributor to non-linear factors in this case, is fairly high.

In analyzing particle H, whose experimental and measured distributions are shown in Fig. 2-18 , the factors listed in Table 2-9 essentially predict the outcome of an experimental attempt to measure size distribution. The fact that the test particle pulses are the same size as the noise introduces complications since no method of noise analysis is known. No valid comparison with measured data can be made in this case unless noise variations are taken into account.

Figures 2-19 and 2-20, which display experimental distributions, are difficult to analyze since the signal to noise ratio are below 1 and the effects of the finite size of the light pipe can introduce a larger error. Essentially these results in Fig. 2-19 and Fig. 2-20 showed that small particles which produce pulses below the noise level can be detected.

f) CONCLUSIONS

1) The agreement between the observed size spectrum of glass particle and the measured size spectrum showed that the shadow technique may be used to determine a partially opaque particles spectrum provided the size of the light fibers is small compared to the diameter of the particle, the signal to noise ratio is high (a factor of 3 or greater), and the chance that a particle does not fully intercept the light beam is  $1/3$  or less.

2) The occurrence of recorded pulses in Fig. 2-19 and Fig. 2-20 showed that particles can be detected even if their signal to noise ratio is less than one.

3) The size distribution of colored water droplets (sizes range from  $20\mu$  to  $60\mu$ ) from an atomizer have not been determined at this time, but the shadow technique offers promise for this size distribution measurement if the suggested improved probe can be built.

4) Since the water spray was not accurately measured final judgements concerning the applicability of the shadow technique should be delayed until better equipment is obtained.

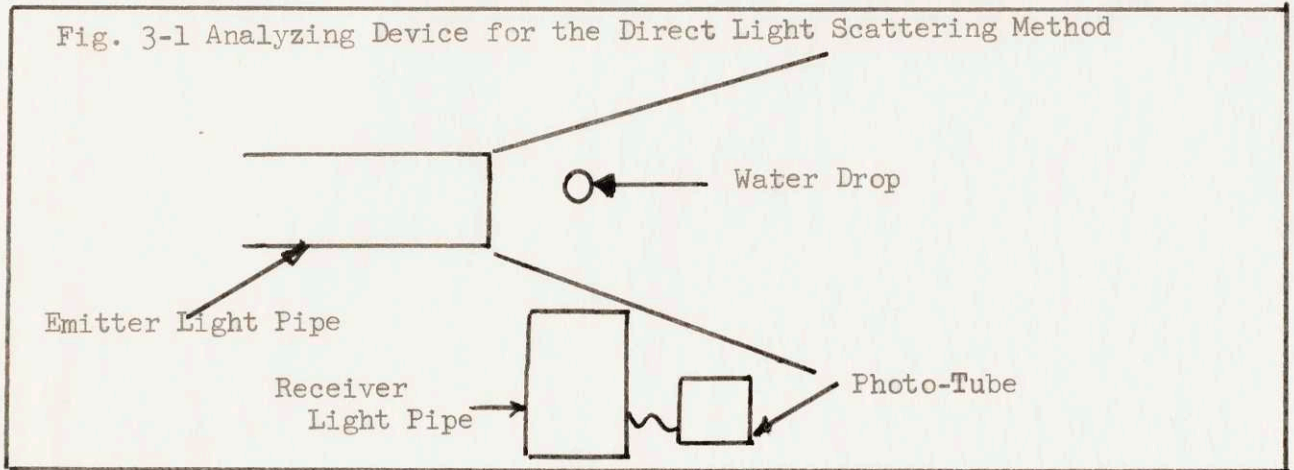
Chapter III

The Light Scattering Method

a.) Theory

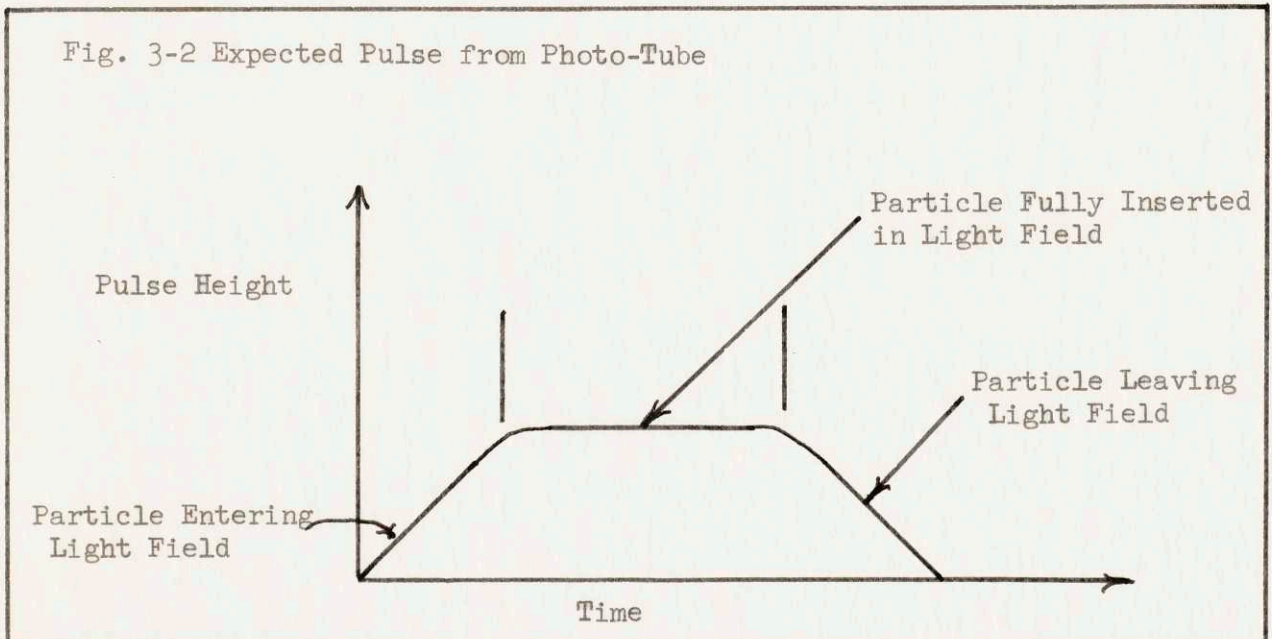
Figure 3-1 shows the essence of the apparatus needed for measuring the light scattered by a test particle. This device consists of a receiver light pipe and an emitter light pipe arranged so that the receiver light pipe does not intercept the light beam from the emitter pipe. A water particle traveling through the light

Fig. 3-1 Analyzing Device for the Direct Light Scattering Method



field reflects light into the receiver pipe and connected photo-multiplier tube. Subsequent analysis of the photo-multiplier signal, depicted in Fig 3-2, can yield information regarding particle size, density, and velocity.

Fig. 3-2 Expected Pulse from Photo-Tube





This pulse exhibits a rise portion when the particle enters the light field, a middle non-flat portion when the particle is fully contained in the light field and a descending portion when the particle leaves the light field. The shape of the middle portion of the observed pulse is not known, however it is unlikely that this portion is flat. The entire pulse shape strongly depends upon the geometrical relation between the test particle, the receiver light pipe and the emitter light pipe.

The maximum observed pulse height is expected to yield information concerning the radius of the particle. The total time duration of the pulse can yield information concerning the particle velocity if the particle's path length in the light field is known, since the particle velocity is just the total path length divided by the total time duration of the pulse. The frequency of pulses can yield information concerning particle density or flux distribution if the shape of the light field which effectively scatters light into the receiver light pipe is known. The light pipes will accept or emit only light which strikes or is emitted from the front surface of the pipes at an angle of  $22\frac{1}{2}^{\circ}$  or less. This angle is measured from the normal of the light pipe frontal surface to the path of the incoming or outgoing light ray. Hence the effective volume of light scattering is that bounded by the intersection of the cone of light from the emitter pipe and the  $45^{\circ}$  cone from the receiver pipe.

An estimate of the quantity of light scattered by the test object and collected by the receiving system is desirable to determine whether the electrical pulses produced from the collection of this scattered

ray. Hence the effective volume of light scattering is that bounded by the intersection of the cone of light from the emitter pipe and the  $45^{\circ}$  cone from the receiver pipe.

An estimate of the quantity of light scattered by the test object and collected by the receiving system is desirable to determine whether the electrical pulses produced from the collection of this scattered light are larger than those produced by the noise levels of the counting equipment. This amount of scattered light can be determined by knowing the relative geometry between the test object and the light pipes, and by determining the distribution of light scattered by the test object. In the case of water drops the light scattering distribution can be found by using Ref (6,7, and 8).

## b) Apparatus

The equipment for this investigation consists of two light pipes, a light condensing system, a photo tube, a super stable high voltage supply, a linear amplifier, an oscilloscope, a stroboscope, a black box and other miscellaneous equipment. Fig 3-3 shows a typical arrangement of this apparatus.

Light from the stroboscope is condensed and channeled through a light pipe, called the emitter light pipe. This light is partially reflected by a test object and collected by another light pipe attached to a photo-multiplier tube which converts this light signal into an electrical signal . After amplification by a preamplifier and a linear amplifier, the signal can be analyzed by either an oscilloscope or pulse height analyzer.

Table 3-2 lists all standard equipment used for these experiments. The following explains and describes this equipment.

### Light Producing Equipment

A stroboscope was chosen as the light source since this apparatus could produce a more intense light beam than any other easily obtainable source. For comparison purposes with other light sources Table 3-2 is included. The only other man made piece of equipment which can produce light intensities greater than a stroboscope is a laser.

Table 3-1 Table of Standard Equipment

<u>Equipment</u>	<u>Manufacturer</u>
Oscilloscope Model #545 with Type L Plug in Unit	Tetronic Inc., Portland, Oregon
Pulse Height Analyzer with 210 Plug in Unit and 220 Data Output Unit	Technical Measurements, Corp., North Haven, Conn.
Digital Recorder model 561B	Hewlett Bachard Palo Alto, Calif.
Linear Amplifier Model No 218	Baird Atomic, University Rd., Cambridge, Mass.
Super Stable High Voltage Supply Model 312A	Baird Atomic
Preamplifier Model 255	Baird Atomic

Table 3-2(Ref 9.) Comparison of Light Sources

	<u>Tungsten</u>	<u>Zirconium Arc Lamp</u>	<u>Carbon Arc</u>	<u>Sun (Surface)</u>	<u>Strobe *</u>
Brightness <sub>2</sub> Candles/mm	10-25	40-100	175-800	1600	100-1700

\* The intensity of the stroboscope flash was estimated by calibrating the light from the strobe with a standard in order to find the amount of light released per flash of the strobe and by assuming the dimension of this light flash to be a cylinder 2 mm in diameter and 10 mm in length.

### Light Collecting and Condensing Equipment

The purpose of this equipment is to collect the light from the strobe, condense this light, and focus the condensed light on the end of the light pipe. This system is similar to that previously used in the shadow technique and need not be discussed.

Black Boxes - The purpose of these boxes is to prevent reflections by stray objects from being picked up by the receiver light pipe. The box, shown in Fig 3-4, has a hole cut in the front face so that the light might enter. A black cone was placed inside the box to reflect entering light against the black painted interior walls. After successive light reflections from the cone and walls most of the light entering the box would be absorbed with little reflected out. Tests showed that between  $10^{-6}$  and  $10^{-7}$  of the light which entered this box was reflected out.

Electronic - Fig 3-5 displays a block diagram of the electronic set-up.

Fig. 3-3  
Experimental Set Up

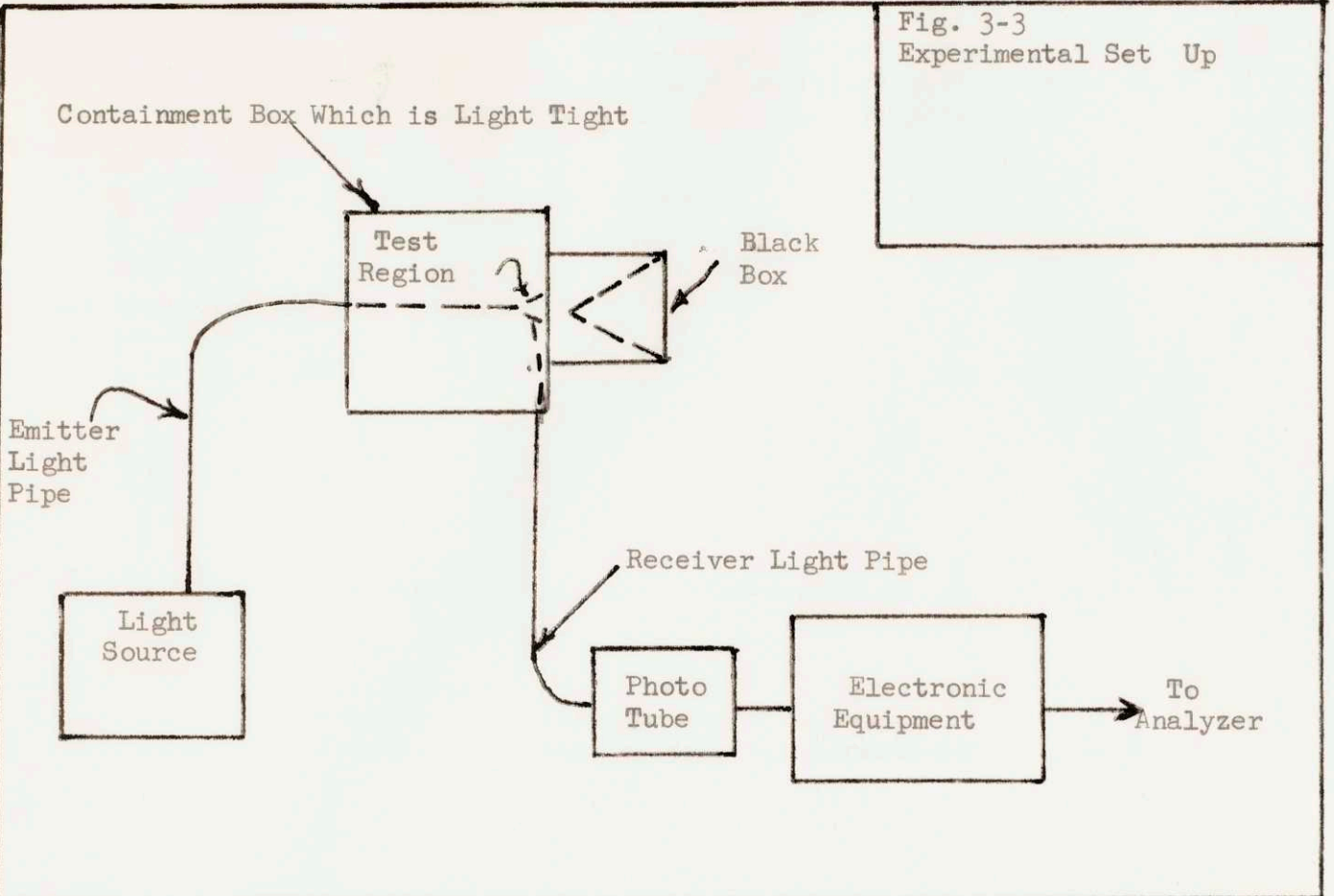
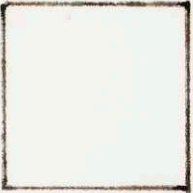
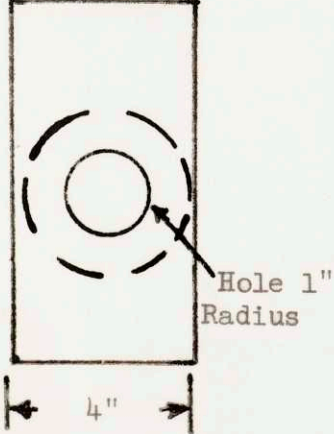


Fig. 3-4  
Black Box

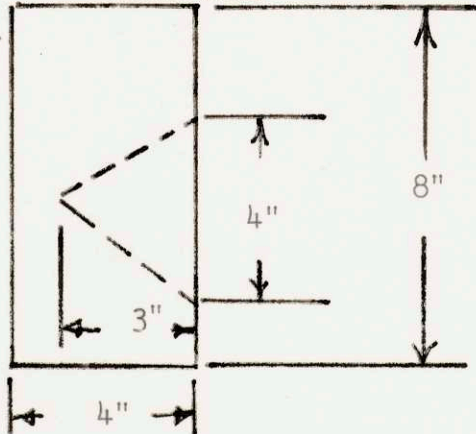
Top View



Front View



Side View



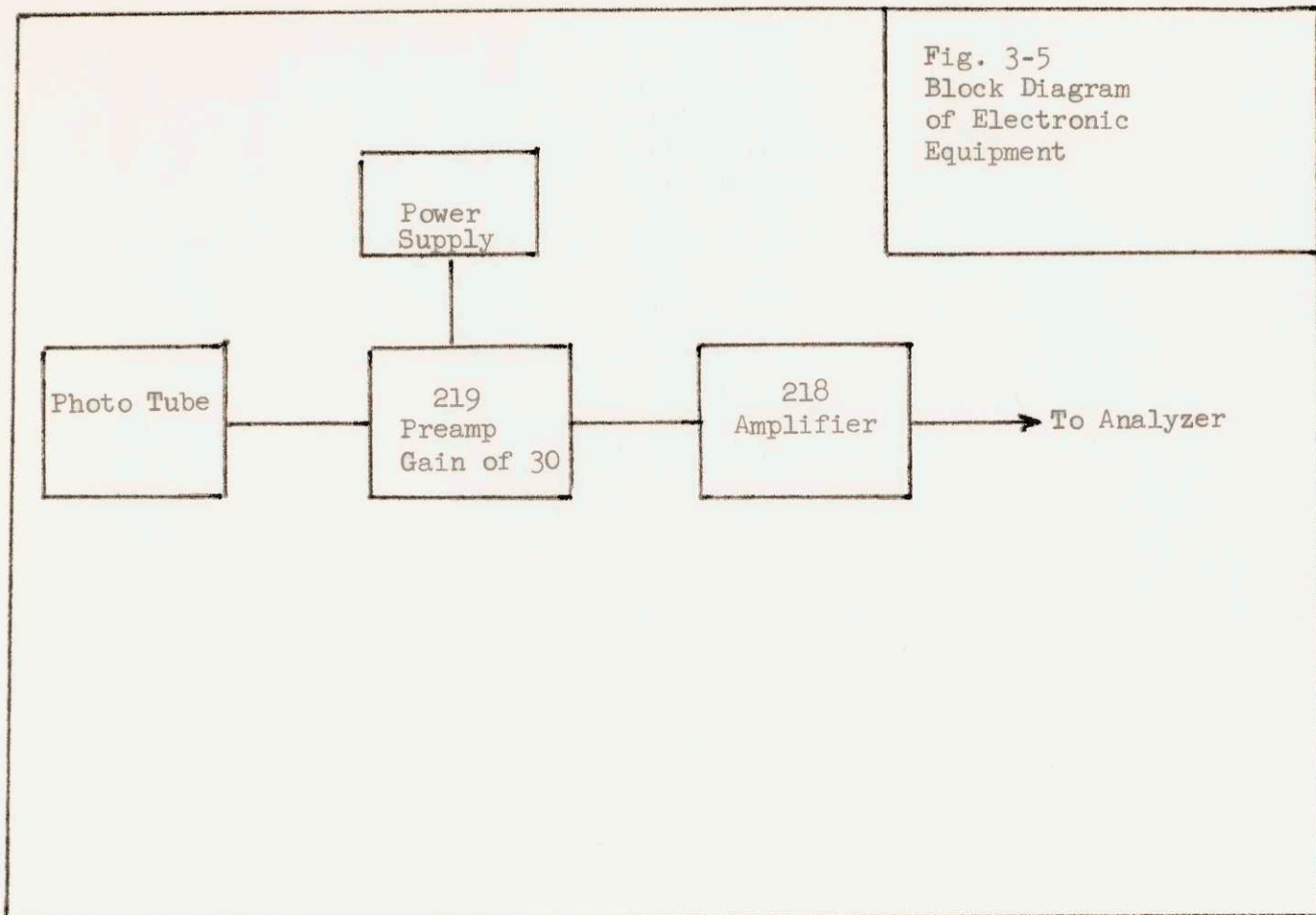


Fig. 3-5  
Block Diagram  
of Electronic  
Equipment



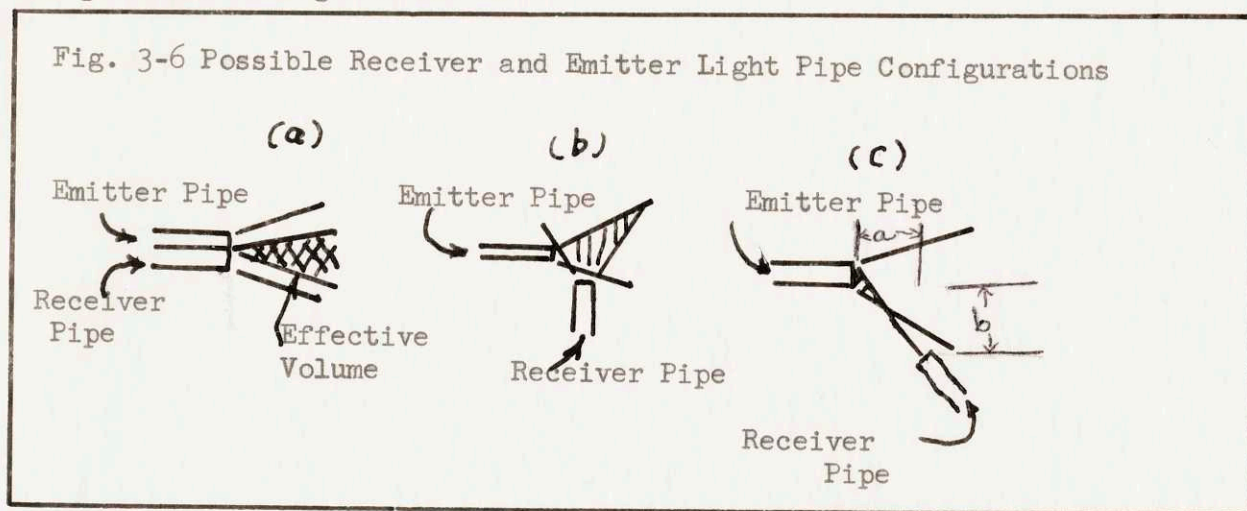
c) Experimental Procedure

The apparatus was arranged as shown in Fig 3-3. The light pipes were arranged as shown in Fig 3-6 and water drops were sprayed into the test region.

d) Experimental Results

Initial experiments as done with the apparatus in Fig 3-3 and the light pipes arranged in configuration a and b of Fig 3-6 pointed out a major difficulty. This difficulty is that single particles cannot be distinguished from groups of particles since the volume of space in which a particle may be detected is large enough to hold several particles at once. Since the light pipes can receive or emit light within a  $45^\circ$  cone angle, the volume generated in space by the intersection of these cones can be quite large.

This volume can be made small enough to contain one particle by arranging the light pipes as shown in configuration c of Fig 3-6. This arrangement also takes advantage of utilizing the much larger forward component of scattered light than the smaller backward component which the previous configurations used.



Although this arrangement circumvents the previous difficulty further problems arise when particles strike the emitter light pipe. These particles either were deformed and bounced or stuck to the end of the emitter pipe.

The inability to effectively scatter and collect light from a single particle terminated these positive light scattering experiments.

e) Discussion and Observations

- 1) The main problem in the determination of size by measuring the light scattered from a test particle is to keep the volume, formed by the intersection of the cone of light from the emitter with the  $45^{\circ}$  light receptive cone of the receiver light pipe, small enough so that only one particle at a time enters this volume.
- 2) Density or flux measurements are possible provided the geometry of the effective scattering volume is known and is small enough to contain a single particle at a given time.
- 3) Velocity measurements are difficult if not impossible since the effective scattering volume generated in space is not a simple geometric figure and the particle path length varies from particle to particle.
- 4) Placing the light pipes in the position indicated in Fig 3-6 configuration C , seemed to reduce the effective scattering value to a very small zone. However the receiver pipe had to be placed about . 1 cm from the emitter pipe so that the fringing light field accompanying the emitter pipes field had no effect. The placing of the probe 1 cm apart may not be practical in dense fog flow.

f) Conclusion

In view of the statements made in the Discussion and Observations section the possibility of using the direct light scattered from a particle in a dense fog flow seems small if light pipes are used to transmit and receive light.

Chapter IV

Suggestions For Future Work

a) Suggestions for future research and improvement of the "shadow method"

1) Before designing another probe more data concerning particles H, R, and the Spray should be taken. This data should be taken with light pipes whose fiber diameters are about the size of  $1\mu$  and with pipe dimensions which are small enough to obtain a signal to noise ratio greater than 3.

2) Attempts should be made to find a photo tube or photo cell whose noise variations, when a high intensity light strikes the photo cathode, is much smaller than 5% of the total output pulse.

3) A method to analyze the manner in which noise variations affect the observed pulse heights should be sought.

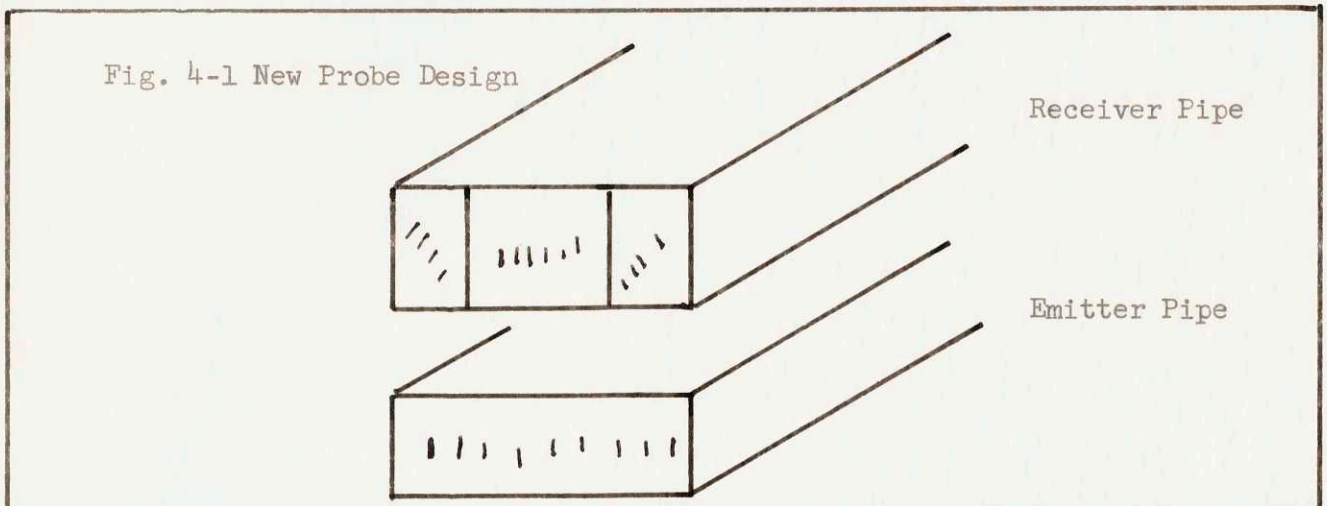
4) A better analysis of the effects listed in Table 2-4 be developed.

b) Suggestion for an improved probe

The following contains a discussion concerning the design of a future probe.

1) New Probe

This probe should minimize or eliminate the chief three non-linear factors: 1) The effect of the finite size of the light pipe fibers, 2) Edge effects and 3) Noise. Figure 4-1 shows the ends of the emitter and receiver light pipe. The mechanical mechanism aligning these pipes in space will not be considered. The following discussion is mainly concerned with the design of the light pipes.



The pipes depicted in Fig. 4-1 consist of a rigid array of very small fibers whose diameter is below  $1\mu$ . Since particle sizes in fog flow are of the order of  $20\mu$  any non-linear effects due to the finite size of the light pipe fibers will be eliminated. The front portion of each pipe contain rigid fibers for the initial few centimeters while the rear portion contain flexible fibers. The emitter pipe contains a single incoherent bundle arranged in a rectangle. The receiver probe contains three distinct regions of fibers separated from each



other. The probe may be constructed of a single rectangular coherent bundle of fibers and the regions formed by separating the fibers at the back end of the receiver pipe. This setup permits varying the dimensions of each rectangular region. The probe may also be constructed of three separate rectangular light pipes stuck together.

Edge effects can be eliminated by the three region probe. Consider the experimental set-up shown in Fig. 4-1 with a colored water spray or number of opaque spheres flowing at different times between the two light pipes. The space between the two pipes is small enough so that only one particle at a time passes between the pipes. Assuming a vertical particle velocity, a particle shadow may take any one of the five paths, shown in Fig. 4-2, as it crosses the receiver pipe. Paths a and b correspond to particles passing only the outer regions of the pipe, paths c and d represent particles crossing both the outer and middle zones, and path e signifies particles crossing only the center zone. The electronics of the system is arranged to record only particles contained fully within the central zone. Particles which enter the outer zones (path a and b) will not be counted. Particles which enter both the central and outer zones path (c and d) produces light pulses from both zones. After photo tubes convert these pulses to electrical pulses, they enter an anti-coincidence system which destroys them. Pulses produced only in the central region can pass the anti-coincidence system and be counted,

Fig. 4-2 Possible Paths a Falling Particle May Take

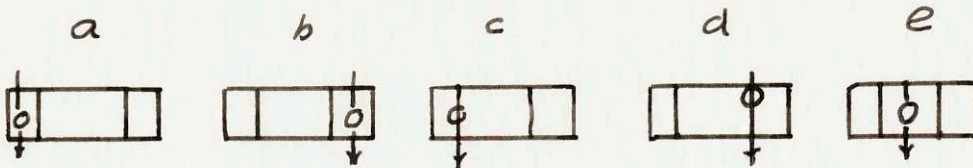
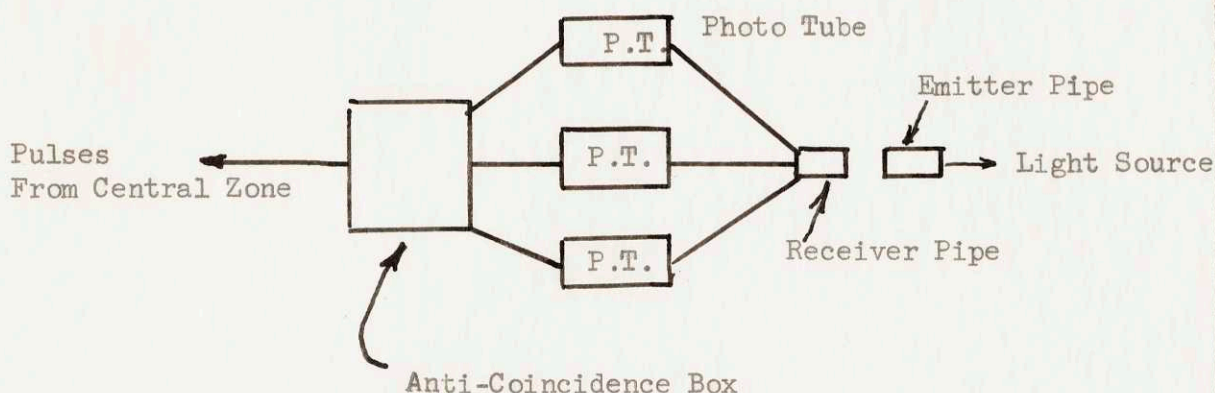


Fig. 4-3 General Electronic Arrangement for New Probe



The size of the central region is a critical dimension. Two non-linear factors may be introduced depending upon whether the size of this region is much greater or almost the same as the test particles. If this region is much greater than the average particle diameter there is a possibility of having more than one particle in the central region at the same time. If the central region is slightly larger than the test particles, the probability of fully containing a large particle in the central region will be small while the probability of fully containing a small particle in this region will be much greater. Definite consideration should be given to this latter effect in the design of this type of probe and in analyzing any data produced from the probe.

The size of the central portion depends upon the expected size of the test particles. Following is a brief illustration of the method used to determine the dimensions of the central region. Let  $y$  denote the magnitude of the D. C. shift,  $A$  the frontal area of the central region, and  $a'$  the area of the test particle. The photo tube noise variation was found to vary between  $0.025 y$  and  $0.05 y$ . Assume that it is possible

to operate the photo tube at the low value of 0.025 y. The lower limit for accurate signal detection and analysis may be arbitrary set at three times the noise level of 0.075 y. The expected pulse height from the smallest test particle is  $\frac{a}{A}$  y. Setting this quantity equal to 0.075 y yields  $a = 0.075 A$ .

Assuming a square central region and that a particle fully occupies this region. The area of the largest observed test particle  $a_L$  is

$$[a_L = \frac{\pi}{4} \times \frac{a}{0.075} \approx 10a]$$

roughly ten times the area of the smallest particle. The diameter of the largest particle is  $(\sqrt{10} \approx 3.16)$  3.16 times the diameter of the smaller particle. If the smaller particle is  $30\mu$  in diameter the larger would be  $95\mu$ . Since the probability of detecting this particle is very small, the light pipe must be made, rectangular with a height equal to or slightly larger than the maximum diameter particle expected. The basis for selecting this maximum diameter particle depends upon the range of experimental test particles expected. In this example suppose the upper range of diameters was selected as  $70\mu$ ; the maximum length of the central position would be  $130\mu$ .

$$\left[ \frac{a}{0.075} \times \frac{1}{70} \approx \frac{\pi}{4} \times \frac{30^2}{0.075} \times \frac{1}{70} = 130 \right]$$

The magnitude of the noise variations is very important, lower values of this variation would permit a larger probe which can increase the range of test particle sizes encountered.

The size of the two end portions of the light pipe should be small enough so that any particle which casts a shadow on any portion of these pieces will be counted. Very large end portions produce high noise variation which can mask shadows partially cast in this region. A rough criteria for

magnitude of the minimum shadow which can be detected by the end portions is 10% of the area of the smallest particle and that the size of the pulse produced from this shadow equals that of the noise pulse. Based on this 10% criteria, a noise variation whose magnitude is 0.025 of the total light flux entering an end portion, and a  $70\mu$  light pipe height, the width of each end portion can be  $34\mu$ .

The total size of the receiver pipe in the above illustration is  $70\mu \times 198\mu$  which is small enough to fit inside some hyperdermic needles.

## References

1. H.C. Van De Hulst, Light Scattering By Small Particle, John Eiley, New York, 1955
2. F.T. Gucher, C. T. O'Konshi, H. B. Pickard, and J.N. Pitts, Journal of American Chemical Society, 69,2422, 1947
3. F. T. Gucher, and D.G. Rose, British Journal of Applied Physics, Nottingham Conference Supplementary, 1954
4. B. J. Bretter, Photogrammetry The Evaluation and Calibration of Photogrammetric Systems, Edgerton, Germeshausers, and Grier, Boston, Mass, P. 53. Fig. 3-9
5. RCA Electronic 2 Handbook H B -3, Radio Corp. of America, Electronic Tube Div. Commercial Eng. , Harrison, New Jersey
6. Stratton, Electromagnetism , McGraw Hill, New York, 1941.
7. Philips and Panobsky, Classical Electricity and Magnetism, Addison Wesley, Reading, Mass.
8. H.C. Van De Hulst, Chpts 9 and 10, op.cit.
9. William A. Stewart, Systems for Measuring Instantaneous Fluid Velocities Without Interfering With Flow, MIT, Scd Thesis 1959, p.69.